Determining the feasibility of assessing the adequacy and immunophenotype of human breast core needle biopsies using molecular and H&E fluorescence imaging via deep-UV optical microscopy

David James Cooper

A thesis
submitted in partial fulfillment of the
requirements for the degree of

MASTER OF SCIENCE IN BIOENGINEERING

University of Washington
2021

Committee:
Eric J Seibel
Ruikang Wang

Program Authorized to Offer Degree:
Bioengineering

University of Washington

Abstract

Determining the feasibility of assessing the adequacy and immunophenotype of human breast core needle biopsies using molecular and H&E fluorescence imaging via deep-UV optical microscopy

David James Cooper

Chair of the Supervisory Committee:

Eric J Seibel

Department of Mechanical Engineering

Histopathology techniques have not advanced with related technological innovations made in the last few decades. As a result, they are needlessly time consuming, labor intensive, and are not adapted for core needle biopsies (CNBs), an increasingly common, minimally intensive biopsy technique. CoreView, a novel histopathology-on-a-chip device under development in the Seibel Laboratory, can solve these problems by automatically handling and imaging fresh CNBs at the point-of-care. To succeed as a histopathology device, CoreView needs a stock of UV-compatible stains and immunohistochemistry (IHC) biomarkers to enable fresh tissue imaging with deep-UV light. Due to its importance in breast cancer, one of the cancers most frequently biopsied with a core needle, this study focuses on staining the HER2 antigen with a novel UV-compatible biomarker. To assess the biomarker's accuracy and effectiveness in CoreView, fresh human breast cancer specimens and formalin fixed paraffin embedded HER2+ and HER2- tissue slides are imaged. Additionally, each of these tissues undergo gold standard histopathology to compare the amount of HER2 staining and to determine if the stains used in CoreView affect downstream histopathology. Using a novel HER2 IHC score prediction plugin for ImageJ and comparative diagnoses by our collaborating breast cancer pathologist, it was determined that the HER2 biomarker appears to stain the cell membranes of fresh breast cancer biopsies imaged with DUV microscopy. It was also determined that all the stains used to complete this imaging did not disrupt downstream histopathology. For the most accurate conclusion, this biomarker must be tested on a fresh HER2+ breast cancer sample, which was never available during this study. Furthermore, more mechanical work needs to be completed for the CoreView system to produce images a pathologist can use to assess the adequacy of its samples.

ACKNOWLEDGEMENTS

I would first like to thank the CoreView team for the countless hours of support and the resources necessary to complete this master's thesis. My PI, Eric Seibel, introduced me to the CoreView project three years ago, and I am so grateful to have been a part of making this revolutionary device. Mark Fauver provided all the tools I needed this year as my mentor and project lead for my first two years on the team. Matt Carson, who took over for Mark, helped me a lot with the MUSE hardware when problems arose. I am also honored to have helped mentor and train four new undergraduate students who joined the CoreView team in the last two years, as it gave me a new understanding of the project and practice working as a project lead.

I would also like to thank all the collaborators who have helped make this thesis successful. Dr. Suzy Dintzis has provided very valuable advice and put aside time from her busy schedule as a breast cancer pathologist to evaluate almost 70 MUSE, Virtual H&E, and standard histopathology images. Brian Johnson and the Histology and Imaging Core (HIC) have also performed standard histopathology on all the fresh human breast cancer specimens I have received. I would also like to thank NW Biospecimen for providing these human specimens from consenting patients at UW Medicine. Additionally, Richard Levenson and his lab at UC Davis have lent us the MUSE system and the MUSE-to-Virtual H&E colormapper application and provided much needed guidance during this project.

Lastly, I would like to thank my family for the emotional and financial support I needed to complete my 1-year master's thesis. I am blessed to such a caring family, from Jeani, my newly made wife and life partner, and our cats, Gatsby & Lucifer, who give me the love I need every day, to my parents and in-laws, who have paid for much of my living and academic expenses over the years. Without the support of my family, getting my master's education and degree would have been impossible.

In addition to the individual support described above, I would also like to acknowledge the sources of funding that contributed to my thesis project. Through Eric Seibel, I have received funding by the Washington Research Foundation Phase 1 award and the National Cancer Institute Exploratory R21 CA 246359 award.

CONTENTS

Page

List of Tables Page

List of Figures **Page**

1. INTRODUCTION

Histopathology is the diagnosis and study of tissue-scale diseases and is a vital process in the diagnosis of cancer. Histopathology and the technologies used to perform it have not significantly changed for over 75 years, apart from the development of immunohistochemistry in the 1980s[1]. This evolutionary stagnancy of histopathology is similar to that of antibiotics: it worked very well for decades but problems are beginning to amass that can be solved with investments in innovation.

1.1 Current Standards in Pathology

The gold standard of histopathology involves the use of basic light microscopy to take magnified images of stained nuclei, cytoplasm, and other markers of interest. Prior to imaging with the light microscope, four main steps are performed (Figure 1). First, the tissue sample must be fixed to permanently "freeze" the cellular components in their current state[2]. The most common fixative used in histopathology is formalin, an aqueous solution of formaldehyde gas and liquid water[3]. When formalin is exposed to tissue, it binds to uncharged reactive amino groups of proteins and forms cross-links between them. While formalin fixation is reliable and inexpensive, it does have many detrimental aspects. First, formalin is a very dangerous solution that can damage the skin, eyes, and respiratory tract if not handled properly. Second, formalin-mediated cross-linking is non-selective and can result in the unwanted "hiding" of antigens of interest in immunohistochemistry (Figure 3E). Fortunately, there are many antigen retrieval methods that can reverse some of this cross-linking. Lastly, formalin degrades DNA and RNA and can extensively damage proteins[4]. This is a major problem for newer histopathologic techniques such as RNA indexing and other -omics analyses. The entire fixation process takes

around 24-36 hours, depending on the size of the sample, to ensure formalin has penetrated and cross-linked the entire specimen[5].

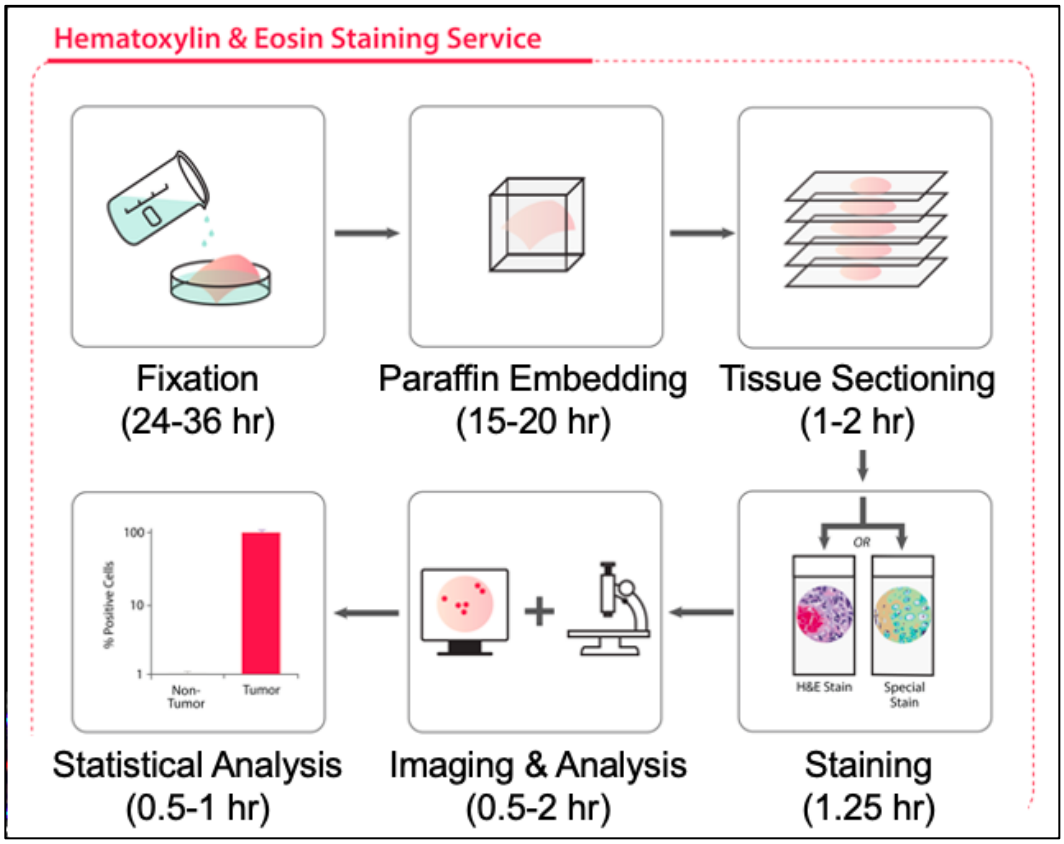

Figure 1 The typical routine of gold standard histopathology. Adapted from abmgood.com[6]

The second step in gold standard histopathology is embedding the fixed specimen with paraffin wax. Paraffin wax is a soft colorless mixture of hydrocarbons derived from petroleum and has an abundance of applications[7]. Paraffin wax's roll in histopathology is to solidify the tissue sample to allow for fine sectioning. As a hydrocarbon, paraffin wax is very hydrophobic and will not infiltrate fixed tissue until a series of dehydrating and clearing steps are performed[8]. This entire process, from dehydration to paraffin embedding, takes 15-20 hours to complete and produces large volumes of waste products[5]. The resulting sample is commonly referred to as Formalin-Fixed Paraffin-Embedded (FFPE) and is fully preserved.

After embedding, the FFPE tissue block must undergo the third step in preparation for imaging: sectioning. Because light microscopy requires very thin (around 5 μm) sections to produce useful, diagnostic-quality images, mechanical slicing of the FFPE block is performed with a machine called a microtome. While automated sectioning exists, most sectioning is still achieved using a manual rotary microtome that requires delicate and skillful labor[9]. Sectioning with a microtome can also produce artifacts as well as reveal ones that were created during fixation or embedding. Once successfully sectioned, the FFPE slice must undergo staining to mark features of interest, such as nuclei and cell membranes. Unfortunately, because most stains are aqueous, the tissue section must be rid of the hydrophobic paraffin wax and rehydrated (step 2 in reverse)[10]. In gold standard histopathology, hematoxylin and eosin (H&E) are the most commonly used stains. After staining, the tissue slice is then mounted onto a glass slide using a mounting medium that seals the coverslip to the tissue and the slide. The combination of sectioning, staining, and mounting can take around 2-3 hours to complete, and are the final steps in the tissue processing of gold standard histopathology[5].

In addition to gold standard H&E histopathology, further diagnostic information can be gained by analyzing the presence of certain proteins with a process called immunohistochemistry (IHC). IHC is a standard histopathological technique used to diagnose cancer because it identifies subtypes that can have very different risks of progression, response to treatment, and survival outcomes. Current IHC also requires FFPE sections to be deparaffinated and hydrated prior to staining. However, it also requires heat-induced antigen retrieval to undo the unselective cross links created during formalin fixation[11]. After antigen retrieval, protein blocking can also be employed to minimize off-target staining. This can be achieved with agents such as bovine serum albumin or synthetic peptides. Lastly, staining is achieved using a fluorescent marker

conjugated to a primary or secondary antibody. A primary antibody is a molecule that will bind to the target protein, while a secondary antibody binds to a primary antibody. Most IHC systems conjugate their fluorescent marker to a secondary antibody because it increases the number of bound fluorophores, amplifying the intensity of the staining.

There are three main antigens stained for in breast cancer IHC due to their commonality and importance in prognoses: estrogen receptor (ER), progesterone receptor (PR), and human epidermal growth factor receptor 2 (HER2). After imaging, a pathologist examines the amount of staining to determine whether the sample is positive or negative for the hormone receptor. Positive means there are enough receptors on enough cells to likely respond favorably to targeted treatment while negative means the opposite[11]. Pathologists may also employ a 0 – 3+ scale to expand the oncologist's treatment options. This system relies on the intensity of staining to score the specimen as 0 (negative), 1+ (weak positive), 2+ (moderately positive), or 3+ (strong positive). The American Society of Clinical Oncology/College of American Pathologists (ASCO/CAP) have defined these values according to percentage of cells stained and the uniformity of individual cell staining[12]. Table 1 shows how samples are given an IHC score for the HER2 antigen. While better than the binary positive or negative diagnosis, the difference between two scoring levels is often indistinguishable and can lead to a false diagnosis. Furthermore, current stains used in IHC are typically monoclonal antibodies conjugated to conventional organic dyes, which have a lower specificity to their target and a lower fluorescence intensity[13]. Moreover, tumor heterogeneity, a common characteristic of breast cancers, can also affect HER2 scoring. Combined, these problems can cause a pathologist to diagnose cancers with a lower IHC score than they should, which can have major implications for patient outcomes.

HER2 status	HER2 score	Amount of Staining
positive	3+	> 10% of cells with uniform intense membrane staining
equivocal	2+	> 10% of cells with incomplete or weak membrane staining OR ≤ 10% of cells with intense membrane staining
negative	1+	> 10% of cells with faint incomplete membrane staining
	0	≤ 10% of cells with faint staining OR no staining

Table 1 Summary of ASCO/CAP HER2 IHC scoring. Adapted from Nitta et al., 2016[12]

In addition to the destructiveness to fresh tissue and intensiveness of labor, current histopathology practices are not optimized for core needle biopsies (CNBs). CNBs have become the preferred biopsy technique for many organs, including breast, due to their minimal invasiveness[14]. The CNB technique relies on a small cylindrical needle that is inserted, often guided by ultrasound, into the tumor. Once inserted, the needle acquires a 5-25-mm-long core of tissue and is removed for histopathological analysis. Despite the increasing popularity of CNBs, very few companies and laboratories have adapted their histopathology routine. As a result, multiple CNBs are required to produce a large enough paraffin block to receive sufficient biological yields after sectioning. This lack of optimization increases the chance of an adverse health event occurring as well as the amount of patient stress by requiring the clinician take more CNBs than necessary.

1.2 Importance of HER2 Over-expression & Diagnosis

The human epidermal growth factor receptor 2 (HER2) is a member of the human epidermal growth factor (HER) family and is encoded by the *ERBB2* proto-oncogene located on the human chromosome 17[15]. All HER proteins are type I transmembrane growth factor receptors whose role are to stimulate cell growth and/or proliferation in response to extracellular ligand binding. While HER2 is normally expressed and present in epithelial cell membranes in low levels (Figure 3B-C)[16], it can transform cells into cancer cells when overexpressed[15]. HER2 overexpression is present in 25-30% of human primary breast cancers and can occur via an

amplification of the *ERBB2* proto-oncogene and/or transcriptional deregulation[17]. These HER2+ breast cancers can have a 40-100-fold increase in HER2 protein expression, resulting in the presence of up to 2 million receptors in the cell membrane at any given time[18]. It is also believed that HER2 amplification is an early event in the transformation into cancer and not a step to activate a later stage[15]. For this reason, HER2+ breast cancer is defined as a subtype and is important to diagnose early.

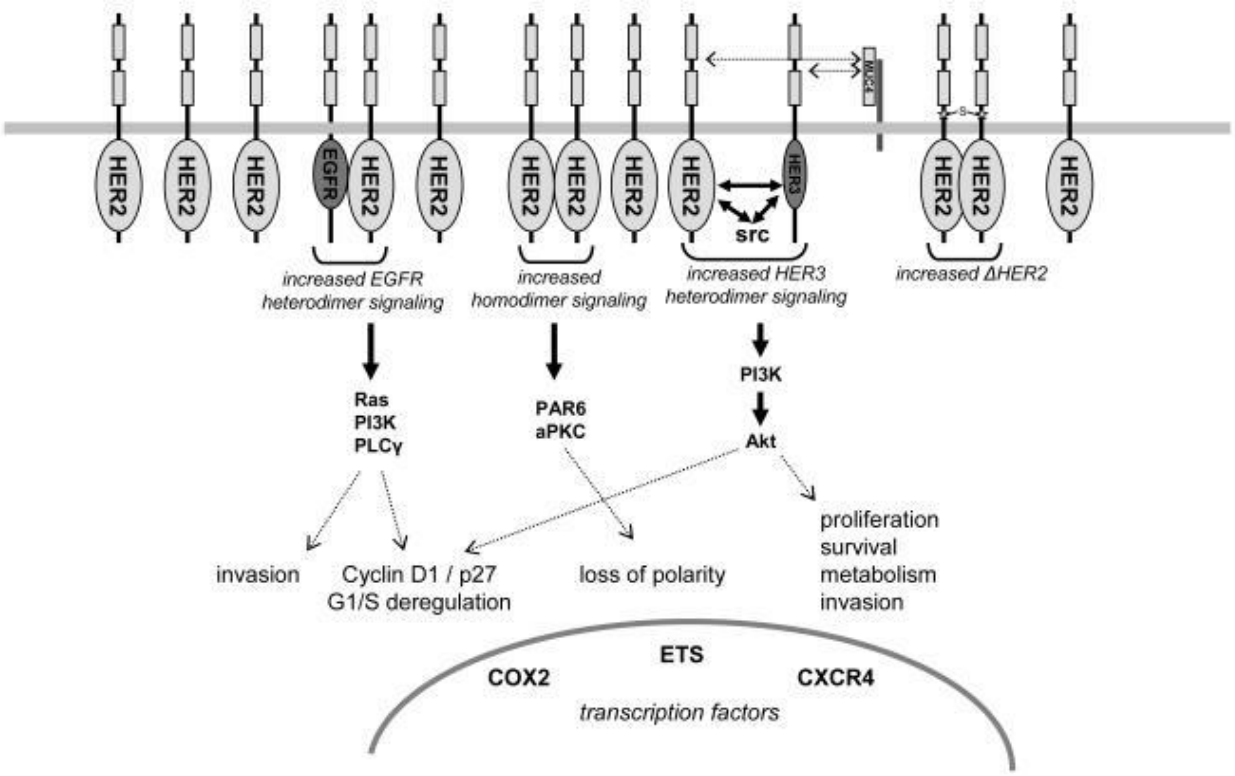

Figure 2 Schematic of the signaling abnormalities resulting from HER2 overexpression and dimerization. From Moasser, 2007[15]

Unlike other members of the HER family, there is no known ligand that binds to the extracellular domain of the HER2 protein[15]. Instead, HER2 activates signaling cascades by forming dimers with itself and other members of the HER family. When HER2 is over-expressed, the likelihood of this dimerization increases substantially. Currently, there are three proposed HER2 dimers that can lead to cellular transformation (Figure 2). The first is the HER2

homodimer, which forms when one HER2 protein binds to another and increases kinase activity and phosphorylation of itself and cellular substrates. Experimentation has shown that this homodimerization can lead to the disruption of tight junctions, loss of cell polarity, and proliferative disarray of breast epithelial cells[19]. The second known HER2 dimer is the HER2-HER1 heterodimer. When HER2 dimerizes with HER1, which is also known as EGFR, it prevents HER1 from undergoing normal endocytic degradation, increasing the amount of HER1 expression and activity[20]. The resulting signal cascades can increase the cell's ability to invade tissues and deregulate multiple steps of the cell cycle, leading to increased proliferation[15]. The third known HER2 dimer is the HER2-HER3 heterodimer. When HER2 dimerizes with HER3, it activates the PI3K/Akt pathway[21], which regulates functions that increase the likelihood of cancer. These functions include cell proliferation and survival, cell size and response to nutrients, metabolism of glucose, cell invasiveness, DNA stability, and angiogenesis[22]. Any of these three HER2 dimers can work alone, or together, to transform a normal cell into a cancer cell.

The HER2 protein and its transformative properties when over-expressed are well studied due to the severity of disease it causes. Early studies of HER2+ breast cancer showed that there is a very strong and significant correlation between *ERBB2* amplification and both time to relapse ($p = <0.0001$) and survival ($p = 0.0011$)[23]. This study also showed that time to relapse and survival are greatly shortened when there are more than 5 copies of the *ERBB2* gene, compared to the normal 1-copy genome. Additionally, HER2+ breast cancers display increased resistance to certain hormonal agents and an increased propensity for metastasis to the brain[24]. For these reasons, it is important to detect and diagnose a HER2+ tumor in its early stage and begin treatment immediately.

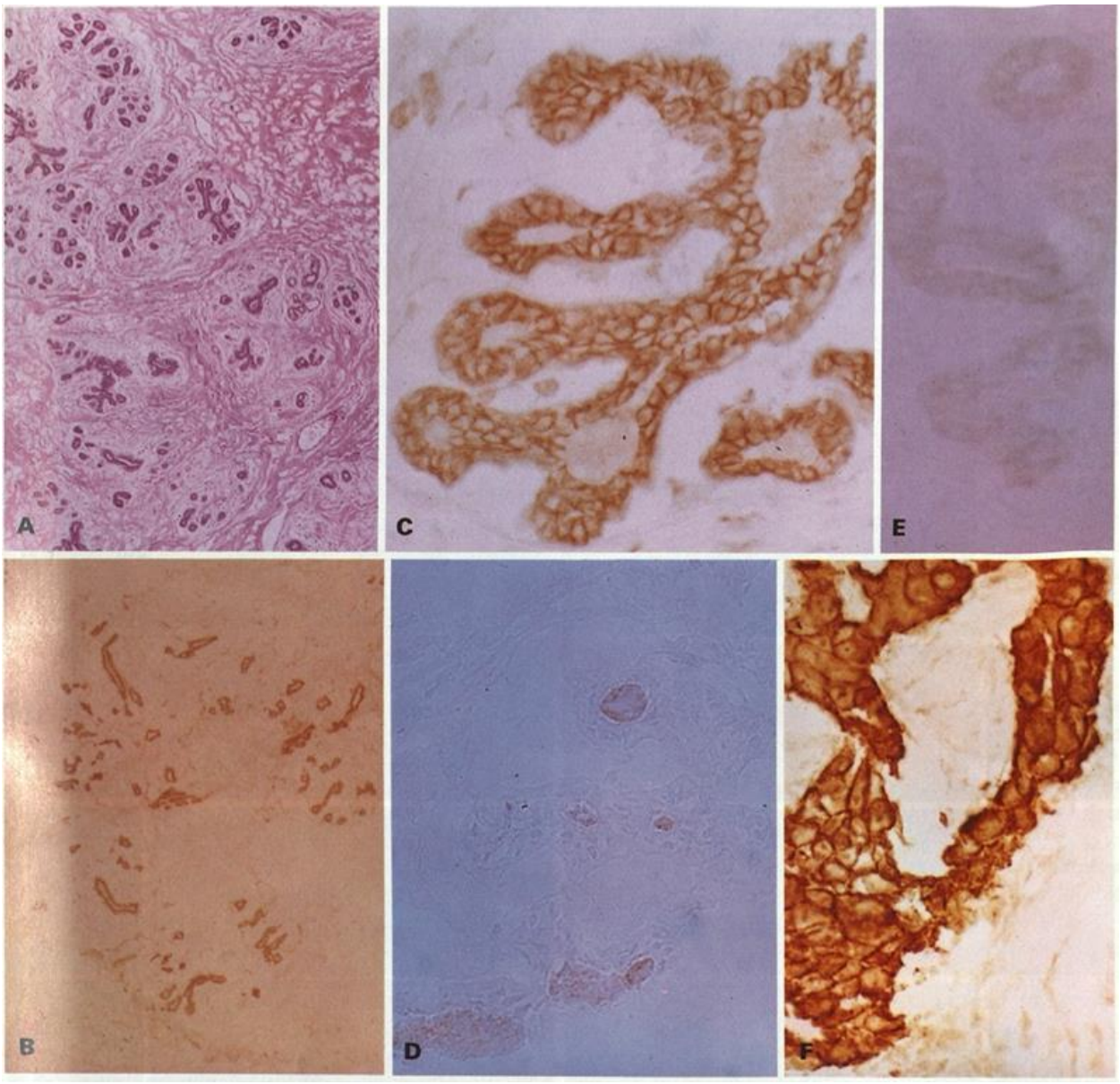

Figure 3 Visual comparison of standard histopathology images of breast tissues with different disease status, HER2 status, and fixation method. (A) H&E stained section of FFPE normal breast tissue showing lobules and ducts. Image was acquired at 150x magnification. (B) HER2 IHC of frozen HER2 2+ breast tissue showing low immunostaining. Image was acquired at 150x magnification. (C) HER2 IHC of a different section of the same sample shown in (B), with increased magnification (1450x). (D) IHC without the HER2 marker used for a negative control of frozen normal breast tissue. Image was acquired at 1450x. (E) The same specimen and imaging protocol used in (C) but fixed in formalin, showing the negative effects of formalin fixation on HER2 IHC. These effects may be somewhat reversed by antigen retrieval, which was not reported used in their methods. (F) HER2 IHC of frozen breast carcinoma with 5-20-fold amplification and overexpression of HER2 (HER2 3+), showing significant membrane staining. Image was acquired at 1450x. (Scanned) from Press et al., 1990[16].

Despite its severity, HER2+ breast cancer has been shown to respond well to targeted treatment with trastuzumab and other drugs. Trastuzumab, sold as Herceptin®, is an anti-HER2 humanized monoclonal antibody that was granted FDA approval in 1998 for metastatic HER2+ breast cancer[25]. Around the same time, multiple studies exploring the effects of HER2 knockdown in cell culture and *in vivo* mouse models showed that HER2+ tumor cells are dependent on HER2 overexpression, and undergo growth inhibition, apoptosis, and tumor regression when HER2 is removed[26-29]. Trastuzumab's function is an analog to the HER2 knockdown explored in these studies; it binds the extracellular domain of the HER2 receptor and induces internalization and degradation via the c-CBL ubiquitin ligase[30]. Additionally, when bound to HER2, trastuzumab can activate natural killer cells through a process called antibody-dependent cellular cytotoxicity (ADCC)[25]. Lastly, the simple binding of trastuzumab to HER2 prevents the occurrence of HER2 dimerization, which suppresses all cellular growth and proliferation caused by the prior HER2 signaling. Combined with chemotherapy, trastuzumab is shown to significantly improve time to relapse and survival in patients with HER2+ breast cancer[31]. Additionally, trastuzumab has a clinical benefit rate of 48% in HER2 IHC 3+ patients and 7% in HER2 IHC 2+ patients. Furthermore, trastuzumab has no effect on HER2- breast cancers, and may actually be detrimental. Therefore, the overexpression of HER2 must be confirmed with IHC prior to HER2-targeted treatment. In all, first-line trastuzumab in combination with chemotherapy has reduced the risk of recurrence of early stage HER2+ breast cancer by 46% and mortality by 33%[32]

Unfortunately, many patients either possess or develop resistance to trastuzumab therapy and require additional HER2-targeted treatments. Current drugs that meet this need include lapatinib (Tykerb®), a dual HER1/HER2 kinase inhibitor FDA approved in 2007, pertuzumab

(Perjeta®), a dual HER2/HER3 monoclonal antibody FDA approved in 2012, and Neratinib (Nerlynx®), an irreversible oral pan-tyrosine kinase inhibitor of HER1, HER2, and HER4 FDA approved in 2017[25]. Additionally, antibody-drug conjugates (ADCs) of trastuzumab covalently linked to chemotherapy agents or inhibitors have been developed to increase the potency of the treatment and reduce off-target cytotoxicity. The last two paragraphs demonstrate how multiple HER2-targeted treatments are available that offer greatly improved patient prognoses when applied to early stage HER2+ breast cancer. Unfortunately, these therapies do not work well on late-stage HER2+ breast cancers and HER2- breast cancers. Combined with the problems experienced in standard IHC histopathology, there is an obvious need for a quicker, easier, and clearer method for diagnosing the HER2 status of breast tumors.

1.3 Microscopy with Ultraviolet Surface Excitation

As discussed in Section 1.1, basic light microscopy used in gold standard histopathology requires very thin sections of tissue to produce clear images a pathologist can use to make a diagnosis. This is the main reason the lengthy, destructive, and labor-intensive FFPE process is required. Fortunately, microscopy with ultraviolet surface excitation (MUSE), developed in the last decade by the Levenson group [University of California, Davis], eliminates this need. MUSE uses deep ultraviolet (DUV) light, around 280 nm, to limit the fluorescence excitation to the surface of the specimen[33-34]. DUV light is absorbed by proteins and stain molecules in cells and the extracellular matrix of the specimen, which prevents tissue below the first few layers of cells from receiving, and thus emitting or reflecting, photons. The MUSE system is used in an inverted microscope geometry, where the objective lens and exciting light are on the same side of the specimen. While more costly and complex than basic light microscopy, MUSE is still much simpler, more robust, faster, and less expensive than alternative optical sectioning

microscopy techniques such as two-photon excitation nonlinear microscopy (NLM) and confocal fluorescence microscopy (CFM)[35].

Since it does not require sectioning, MUSE can be used to image freshly excised tissue specimens. However, because it is such a novel technique, few stains exist that are DUV-excitable[36]. Furthermore, because most stains are created for use in FFPE tissues, which have a degraded plasma membrane, very few of these DUV-excitable stains can readily enter the cells of fresh tissue. As a result, the stains available to stain fresh tissue for imaging with MUSE often do not match the colors used in traditional H&E and IHC histopathology techniques. For example, the nuclear stain, Hoechst 33342, used in this study emits a blueish-green hue while hematoxylin emits a deep blue-purple color. To make it easier for pathologists, the Levenson group has also created an application that takes a MUSE image and converts it into a virtual H&E image (Figure 7)[33]. The application and its process will be discussed in detail in Section 3.3.

1.4 Research Objectives

The principal objective of the research presented in this master's thesis and my capstone report last year is to increase the diagnostic capability of CoreView, the large project encompassing my research that I have been a part of for the last three years. CoreView is a histopathology-on-a-chip millifluidic device that has the ability to stain and image fresh CNBs in under 15 minutes. The principles and main features of CoreView, as well as the work I have put into it during my master's research, will be presented in Section 2. To meet this principal objective, the goal of my master's research is to identify a novel DUV-excitable biomarker that can bind to the HER2 antigen in fresh tissue. This biomarker should also improve the ability to distinguish between HER2 IHC scores, which can likely be achieved by using a biomarker that

has a higher intensity of fluorescence. This biomarker must be rigorously tested with adequate controls and compared to gold standard histopathology to prove that it is a suitable replacement of typical HER2 IHC. Lastly, all stains used for imaging with CoreView-MUSE should not prevent downstream gold standard histopathology after formalin fixation because CoreView is currently intended to function as a preliminary adequacy test on the same CNB that will later be diagnosed using traditional, FDA-approved methods. If shown to be successful, the goals will expand to include the immunostaining of ER and PR with an analog of the novel biomarker used to image HER2 for a more complete breast cancer diagnosis.

The second objective of my master's thesis is to determine if CoreView-MUSE imaging can be used to perform an adequacy test, and if any staining will disrupt downstream histopathology. If CoreView-MUSE *can* perform adequacy tests but the stains required to achieve them prevent the accurate performance of standard histopathology later, the adequacy tests would be pointless because that sample could not be diagnosed. As such, the DUV-compatible fluorescent markers used to stain fresh core needle biopsies for CoreView-MUSE adequacy must be employed for an adequacy test and have their effect on downstream histopathology assessed.

1.5 References

1. Titford M. 2006. A Short History of Histopathology Technique, *Journal of Histotechnology*, 29:2, 99-110. DOI: 10.1179/his.2006.29.2.99
2. Histological Techniques. *Histology Lab Manual*. Columbia University Center for Teaching and Learning. Accessed Jul 12, 2021, from https://histologylab.ctl.columbia.edu/histological_techniques/
3. Chemistry of Formalin Fixation. *News from QED Bioscience*. QED Bioscience. Accessed Jul 12, 2021, from https://www.qedbio.com/blog/chemistry-of-formalin-fixation/
4. Ortega-Atienza S, Rubis B, McCarthy C, Zhitkovich A. 2016. Formaldehyde is a potent proteotoxic stressor causing rapid heat shock factor protein 1 activation and lys48-linked polyubiquitination of proteins. *American Journal of Pathology*. 186:11, 2857-2868. DOI: 10.1016/j.ajpath.2016.06.022

5. Cui Y. 2017. Haematoxylin Eosin (H&E) staining. *protocols.io*. DOI: 10.17504/protocols.io.h8gb9tw
6. H&E and Special Staining. *Histology Services*. Applied Biological Materials Inc. Accessed Jul 23, 2021, from https://www.abmgood.com/H-and-E-and-Special-Staining.html
7. Turner WR, Brown DS, Harrison DV. 1955. Properties of Paraffin Waxes. *Industrial & Engineering Chemistry*. 47:6, 1219-1226. DOI: 10.1021/ie50546a049
8. Embedding. *Histology Lab Manual.* Columbia University Center for Teaching and Learning. Accessed Jul 14, 2021, from https://histologylab.ctl.columbia.edu/histological_techniques/embedding/
9. Sy J, Ang L. 2019. Microtomy: Cutting Formalin-Fixed, Paraffin-Embedded Sections. *Methods in molecular biology.* 1897, 269-278. DOI: 10.1007/978-1-4939-8935-5_23
10. Making histological sections for the light microscope. *What is histology.* The Histology Guide. Accessed Jul 14, 2021, from https://histology.leeds.ac.uk/what-is-histology/histological_sections.php
11. Kim S, Roh J, Park C. 2016. Immunohistochemistry for Pathologists: Protocols, Pitfalls, and Tips. *Journal of pathology and translational medicine*. 50:6, 411-418. DOI: 10.4132/jptm.2016.08.08
12. Nitta H, Kelly BD, Allred C, Jewell S, Banks P, Dennis E, Grogan TM. 2016. The assessment of HER2 status in breast cancer: the past, the present, and the future. *Pathology International*. 66:6, 313-324. DOI: 10.1111/pin.12407
13. Rakovich TY, Mahfoud OK, Mohamed BM, Prina-Mello A, Crosbie-Staunton K, Broeck TVD, Kimpe LD, Sukhanova A, Baty D, Rakovich A, Maier SA, Alves F, Nauwelaers F, Nabiev I, Chames P, Volkov Y. 2014. Highly Sensitive Single Domain Antibody-Quantum Dot Conjugates for Detection of HER2 Biomarker in Lung and Breast Cancer Cells. *ACS Nano*. 8:6, 5682-5695. DOI: 10.1021/nn500212h
14. Pritzker KPH, Nieminen HJ. 2019. Needle Biopsy Adequacy in the Era of Precision Medicine and Value-Based Health Care. *Archives of pathology and laboratory medicine*. 143:11, 1399-1415. DOI: 10.5858/arpa.2018-0463-RA
15. Moasser MM. 2007. The oncogene HER2; Its signaling and transforming functions and its role in human cancer pathogenesis. *Oncogene*. 26:45, 6469-6487. DOI: 10.1038/sj.onc.1210477
16. Press MF, Cordon-Cardo C, Slamon DJ. 1990. Expression of the HER-2/neu proto-oncogene in normal human adult and fetal tissues. *Oncogene*. 5:7, 953-962
17. Slamon DJ, Godolphin W, Jones LA, Holt JA, Wong SG, Keith DE, Levin WJ, Stuart SG, Udove J, Ullrich A, et al. 1989. Studies of the HER-2/neu proto-oncogene in human breast and ovarian cancer. *Science*. 244:4905, 707-712. DOI: 10.1126/science.2470152
18. Venter DJ, Tuzi NL, Kumar S, Gullick WJ. 1987. Overexpression of the c-erbB-2 oncoprotein in human breast carcinomas: immunohistological assessment correlates with gene amplification. *Lancet*. 2:8550, 69-72. DOI: 10.1016/s0140-6736(87)92736-x
19. Muthuswamy SK, Li D, Lelievre S, Bissell MJ, Brugge JS. 2001. ErbB2, but not ErbB1, reinitiates proliferation and induces luminal repopulation in epithelial acini. *Nature Cell Biology*. 3:9, 785-792. DOI: 10.1038/ncb0901-785
20. Huang G, Chantry A, Epstein RJ. 1999. Overexpression of ErbB2 impairs ligand-dependent downregulation of epidermal growth factor receptors via a post-transcriptional mechanism. *Journal of cellular biochemistry*. 74:1, 23-30

21. Soltoff SP, Carraway KL, Prigent SA, Gullick WG, Cantley LC. 1994. ErbB3 is involved in activation of phosphatidylinositol 3-kinase by epidermal growth factor. *Molecular Cell Biology*. 14:6, 3550-3558. DOI: 10.1128/mcb.14.6.3550-3558.1994
22. Vivanco I, Sawyers CL. 2002. The phosphatidylinositol 3-Kinase AKT pathway in human cancer. *Nature Review Cancer*. 2:7, 489-501. DOI: 10.1038/nrc839
23. Slamon DJ, Clark GM, Wong SG, Levin WJ, Ullrich A, McGuire WL. 1987. Human Breast Cancer: Correlation of Relapse and Survival with Amplification of the HER-2/neu Oncogene. *Science*. 235:4785, 177-182. DOI: 10.1126/science.3798106
24. Gabos Z, Sinha R, Hanson J, Chauhan N, Hugh J, Mackey JR. 2006. Prognostic significance of human epidermal growth factor receptor positivity for the development of brain metastasis after newly diagnosed breast cancer. *Journal of Clinical Oncology*. 24:36, 5658-5663. DOI: 10.1200/JCO.2006.07.0250
25. Kreutzfeldt J, Rozeboom B, Dey N, De P. 2020. The trastuzumab era: current and upcoming targeted HER2+ breast cancer therapies. *American Journal of Cancer Research*. 10:4, 1045-1067
26. Colomer R, Lupu R, Bacus SS, Gelmann EP. 1994. erbB-2 antisense oligonucleotides inhibit the proliferation of breast carcinoma cells with erbB-2 oncogene amplification. *British journal of cancer*. 70:5, 819-825. DOI: 10.1038/bjc.1994.405
27. Roh H, Pippin J, Drebin JA. 2000. Down-regulation of HER2/neu expression induces apoptosis in human cancer cells that overexpress HER2/neu. *Cancer Research*. 60:3, 560-565
28. Faltus T, Yuan J, Zimmer B, Kramer A, Loibl S, Kaufmann M, Strebhardt K. 2004. Silencing of the HER2/neu gene by siRNA inhibits proliferation and induces apoptosis in HER2/neu-overexpressing breast cancer cells. *Neoplasia*. 6:6, 786-795. DOI: 10.1593/neo.04313
29. Choudhury A, Charo J, Parapuram SK, Hunt RC, Hunt DM, Seliger B, Kiessling R. 2004. Small interfering RNA (siRNA) inhibits the expression of the HER2/neu gene, upregulates HLA class I and induces apoptosis of HER2/neu positive tumor cell lines. *International Journal of Cancer*. 108:1, 71-77. DOI: 10.1002/ijc.11497
30. Vu T, Claret FX. 2012. Trastuzumab: updated mechanisms of action and resistance in breast cancer. *Frontiers in Oncology*. 2:62. DOI: 10.3389/fonc.2012.00062
31. Vogel CL, Cobleigh MA, Tripathy D, Gutheil JC, Harris LN, Fehrenbacher L, Slamon DJ, Murphy M, Novotny WF, Burchmore M, Shak S, Stewart SJ, Press M. 2002. Efficacy and safety of trastuzumab as a single agent in first-line treatment of HER2-overexpressing metastatic breast cancer. *Journal of Clinical Oncology*. 20:3, 719-726. DOI: 10.1200/JCO.2002.20.3.719
32. Dobson R. 2005. Trastuzumab halves risk of recurrence of breast cancer in some women. *BMJ*. 331:986. DOI: 10.1136/bmj.331.7523.986-d
33. Fereidouni F, Harmany ZT, Tian M, Todd A, Kintner JA, McPherson JD, Borowsky AD, Bishop J, Lechpammer M, Demos SG, Levenson R. 2017. Microscopy with ultraviolet surface excitation for rapid slide-free histology. *Nature Biomedical Engineering*. 1:12, 957-966. DOI: 10.1038/s41551-017-0165-y
34. Qorbani A, Fereidouni F, Levenson R, Lahoubi SY, Harmany ZT, Todd A, Fung MA. 2018. Microscopy with ultraviolet surface excitation (MUSE): A novel approach to real-time inexpensive slide-free dermatology. *Journal of cutaneous pathology*. 45:7, 498-503. DOI: 10.1111/cup.13255

35. Yoshitake T, Giacomelli MG, Cahill LC, Schmolze DB, Vardeh H, Faulkner-Jones BE, Connolly JL, Fujimoto JG. 2016. Direct comparison between confocal and multiphoton microscopy for rapid histopathological evaluation of unfixed human breast tissue. *Journal of Biomedical Optics*. 21:12, 126021
36. Cell Stains & Dyes for Live & Fixed Cells. *Cellular Stains*. Biotium. Accessed Jul 23, 2021, from https://biotium.com/technology/cellular-stains/

2. COREVIEW: A NOVEL MILLIFLUIDIC HISTOPATHOLOGY-ON-A-CHIP DEVICE FOR RAPID ONSITE ADEQUACY ANALYSIS

2.1 CoreView Basics

CoreView is a novel millifluidic system designed to automate the entire histopathology process from acquisition of a CNB to imaging and/or preparation for downstream analysis[37]. The millifluidic chip used in the CoreView system features sequential modules for biopsy removal from the procurement device, transport between modules, staining and rinsing, optical imaging, segmentation, storage, and removal (Figure 4). The system is also designed to be used with any crude or advanced optical microscope designed for thick-tissue 3D imaging, including MUSE. This system is unique in its ability to rapidly and nondestructively handle fresh CNBs for histopathology. Furthermore, custom bidirectional pulsatile flows enable precise transport and staining of these biopsies for the future clinical purposes of performing rapid onsite adequacy in seconds and slide-free histology in minutes.

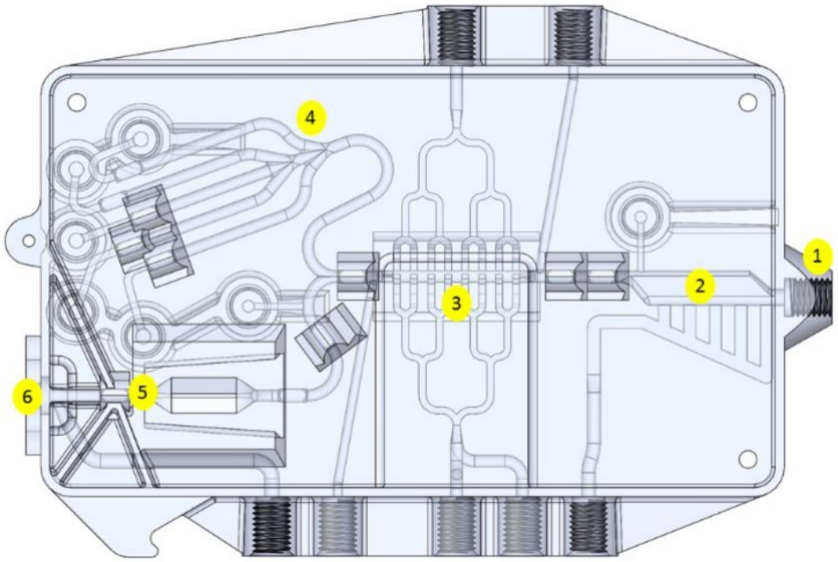

Figure 4 Computer-aided design of a potential final version of the CoreView cartridge. This model features (1) a port for needle insertion, (2) the biopsy removal module, (3) a chamber for staining and rinsing, biopsy rotation, and imaging, (4) the multiplexed storage "parking" module, (5) the biopsy segmentation module, and (6) an exit port for biopsy removal from the chip.

The ability of CoreView to accurately and nondestructively transport fresh CNBs, and any associated tissue fragments, is a result of plug-like flow. Plug-like flow is characterized by a flat velocity profile across the circular cross-section of a cylindrical tube and is achieved by using small fluidic pulses with a high frequency and a short rise time[38-40]. Although these plug-like flows produce precise and regular distances of biopsy movement during transport, the high-shear, parabolic flow used to remove the biopsy from its needle does not. As a result, the movement of the CNB off its needle and into the transport tube is unpredictable and simple automation of the system using a specified number of pulses is unattainable. To enable automation, we have also developed a biopsy tracking MATLAB-based application that can detect and determine the spatial location of a biopsy, its potential fragments, and any air bubbles in real time. Our vision for CoreView is to have a clinician acquire a CNB from a patient and immediately insert the needle into the cartridge. Then, the CoreView system automates the entire (fresh biopsy) histopathology process without input from the clinician, besides hitting a start button.

If successful, CoreView has the potential to revolutionize histopathology. Unfortunately, current inexpensive microscopy technologies make it difficult for CoreView to produce images of relevant diagnostic quality[41]. As a result, the current plan is for CoreView to function as a rapid onsite evaluation (ROSE) adequacy test to ensure the CNB successfully acquired tumor cells. While this does not require immunophenotyping, it will require the use of the Hoechst nuclear stain and Rhodamine B cytoplasmic stain, well studied in my capstone research, and the virtual H&E software used in my master's thesis project. Still functioning as a ROSE adequacy device, CoreView can also segment a biopsy for placement in different media for downstream

pathology tests, such as formalin for histopathology and RNAlater for RNA indexing and other genomics evaluations.

2.2 2020-2021 Contributions

For most of the 2020-2021 academic year, I have worked on the CoreView project in a supporting role. While I was waiting for supplies to ship during the Autumn 2020 quarter, I was assisting the project lead, Mark Fauver, with most of his CoreView experiments as he was preparing to leave the lab to work in industry. The experiments that consumed the majority of my time were designed and performed to assess the functionality and reliability of the biopsy removal module (Appendix I). In these biopsy removal experiments, a CNB was acquired from a section of porcine tissue, donated from pig experiments performed at the University of Washington Center for Industrial and Medical Ultrasound, and placed in either the proof-of-concept removal module or the integrated CoreView cartridge. Then, pressure-driven millifluidic pulses were applied in sequences of increasing pressure until the tissue core was removed from the needle. Because it is important that the tissue is non-destructively transported by CoreView, the intactness of the CNB was monitored at all times during biopsy removal. With these experiments, I found that the biopsy removal module, alone and integrated into the CoreView cartridge, is very successful and reliable at quickly and non-destructively removing a fresh CNB, of different sizes and organs, from its needle (Table 2).

Tissue	Needle Gauge	N	Removed from Needle	Biopsy Stayed Intact	Removal Pressure (psi)		
					Mean	Median	Std. Dev.
Breast	14	20	100%	90%	3.5	3.0	1.93
Lung	14	20	100%	95%	3.1	3.0	1.21
Pancreas	14	20	100%	94%	3.5	2.0	2.33
Kidney	14	30	100%	100%	2.8	2.0	1.45
	16	10	100%	100%	3.2	3.0	1.40
	18	10	100%	80%	5.4	5.0	2.67

Table 2 Experimental results of the biopsy removal experiments show that the module successfully and reliably removes fresh CNBs. All tissue used in these tests came from a freshly resected porcine organ.

When Mark Fauver left the lab, I took on more supportive responsibilities for the CoreView project. Of these, my principal duty was to manufacture all 3D printed parts using our 3D printer [Form 3, Formlabs]. The Form 3 printer is a low force stereolithography printer that

adds resin to an elevating platform by curing a single point at a time. For most prints, we use Formlabs' Standard Clear resin, which prints and cures optically clear to allow for a visual assessment of the biopsy's position during all CoreView functions. During the 2020-2021 academic year, I have printed over 20 CoreView cartridges, 10 accessory parts, 3 proof-of-concept biopsy segmentation, and a couple parts for myself. Each print requires multiple post-print processing steps, beginning with a wash with isopropyl alcohol (IPA) for six minutes to remove uncured resin. Next, supports added to ensure an accurate print are removed using wire cutters. This is one of the most labor-intensive steps of the post-print processing because it requires delicate and precise cutting to ensure all supports are cleared and no features of the print are damaged. After removing the supports, the print is soaked in IPA for a second time to remove pieces of the supports that may have been left behind. If the print has an internal channel with a screw-fit port, like the CoreView cartridge, it must undergo two additional steps. First, the ports must be tapped using a T-handle tap wrench (Dreamcolor). During this step, care must be given to avoid clogging the channel with resin shed during tapping. While this could be avoided by tapping after curing the print, I have found that curing increases the brittleness of the print and tapping frequently causes the port to snap off. After tapping, an IPA rinse is applied using a syringe to identify any blocked channels as well as clear all open channels of resin debris. If there *are* blocked channels, additional rinses with methanol, ethanol, and/or acetone may dissolve the blockage. However, it the channels were blocked during printing, they will most likely be cured and are nearly impossible to resolve. If the print has been successfully tapped and cleared of debris, it is then dried using an air compressor to allow for an easier cure and to fully ensure there is no leftover resin debris inside the channels. The last step for all prints is curing with UV light and heat. The entire post-print processing is time consuming and labor-intensive, with small prints taking around 30-45 minutes to complete and large prints, such as the CoreView cartridge, around 1-2 hours.

In addition to performing all 3D printing duties, I have also contributed to CoreView with my assistance to and training of the undergraduate students on the project. During the Autumn and Winter terms, I assisted Dylan Klavins, a Junior in Mechanical Engineering, with building and testing his proof-of-concept biopsy segmentation module. For this, I 3D printed over 30 individual parts for 3 iterations of the device. I also provided fresh porcine CNBs and videography assistance during the testing of the module. In addition to this brief work helping

Dylan, I was able to gain valuable experience training new undergraduate students in the Spring and Summer terms. Two new students, Tammy Luu, rising Senior in Chemical Engineering, and Kaitlin Danh, rising Sophomore, undeclared, joined the lab in the Winter term and began in-person work at the end of the Spring term. As the only graduate student on the project, I oversaw training them on all aspects of CoreView, including the millifluidics software and hardware, 3D printing, and the biological basis of the project. In addition to training, I also assisted them in the first three weeks of their individual projects to ensure they had a strong start and could make their work successful.

Lastly, in May of 2021 I had the honor of writing the majority of the first manuscript, for publication, detailing CoreView; the need, its functions, and the implications for pathology. There have been a couple conference papers on certain modules, such as the biopsy removal device, but there has not been a paper devoted to the entire CoreView system. To write this manuscript, I had to learn aspects of the CoreView project I was not experienced with, such as the biopsy tracking application and the physics of plug-like flow, in addition to summarizing all my knowledge on the project. This was an extremely stressful process, as I had a week to complete the first draft but made me feel very satisfied and accomplished upon its completion. After extensive editing, the CoreView manuscript[37] was submitted to Lab on a Chip on May 31, 2021. Unfortunately, the paper in its current form was rejected from publication but strongly encouraged to resubmit after addressing the comments from the peer reviewers. We plan to resubmit the edited paper before September 1, 2021.

2.3 Relevant Future Work

The work highlighted in this master's thesis, and my previous capstone report, is essential for the diagnostic success of CoreView. As mentioned previously, CoreView is currently intended to serve as a ROSE adequacy test to determine if a CNB successfully acquired a section of the tumor. To accomplish this the CNB must be stained with UV-excitable, fresh-tissue-compatible biomarkers determined adequate by my research. Additionally, we are being considered for an NIH R21 global health grant to use CoreView in low-resource settings of low-income countries, specifically in Africa, to perform breast cancer histopathology, including HER2 IHC. Breast cancer is the most common cancer and second leading cause of cancer-related deaths in sub-Saharan Africa[42]. CoreView is perfect for this setting because there are very few pathology laboratories in low-income countries, so diagnosing cancers is incredibly

challenging[43]. Furthermore, for settings that do have pathology laboratories, getting patients to attend follow-up appointments can be difficult, as there is often little transportation infrastructure and clinics can be miles away. Applying CoreView in this setting to take diagnostic histopathologic images of fresh CNBs will eliminate both the need for a nearby pathology laboratory and the need to schedule a follow-up appointment to give a determined diagnosis. This future application of CoreView is directly tied to the research conducted for my master's thesis and will not be successful if I cannot find suitable biomarkers for the HER2, ER, and PR antigens.

2.4 References

37. Cooper D, Huang C, Klavins D, Fauver M, Carson M, Fereidouni F, Dintzis S, Galambos C, Seibel E. 2021. CoreView: Fresh Tissue Biopsy Assessment at the Bedside Using a Millifluidic Imaging Chip. *ChemRxiv*. *Cambridge: Cambridge Open Engage*; This content is a preprint and has not been peer-reviewed. DOI: 10.26434/chemrxiv.14702199.v1
38. Hale JF, McDonald DA, Womersley JR. 1955. Velocity profiles of oscillating arterial flow, with some calculations of viscous drag and the Reynolds number. *Journal of Physiology*. 128:3, 629-640. DOI: 10.1113/jphysiol.1955.sp005330
39. Tsangaris S, Stergiopulos N. 1988. The inverse Womersley problem for pulsatile flow in straight rigid tubes. *Journal of Biomechanics*. 21:3, 263-266. DOI: 10.1016/0021-9290(88)90176-5
40. San O, Staples A. 2012. An improved model for reduced-order physiological fluid flows. *Journal of Mechanics in Medicine and Biology*. 12:3, 1250052. DOI: 10.1142/S0219519411004666
41. Xie W, Chen Y, Wang Y, Wei L, Yin C, Glaser AK, Fauver ME, Seibel EJ, Dintzis SM, Vaughan JC, Reder NP, Liu JTC. 2019. Microscopy with ultraviolet surface excitation for wide-area pathology of breast surgical margins. *Journal of Biomedical Optics*. 24:2, 026501. DOI: 10.1117/1.JBO.24.2.026501
42. The burden of cancer is substantial in every country worldwide, regardless of level of development. *The Cancer Atlas*. Cancer.org. Accessed May 23, 2021, from http://canceratlas.cancer.org/the-burden/sub-saharan-africa/
43. African Strategies for Advancing Pathology. *Survey Data*. Pathology in Africa. Accessed May 23, 2021, from http://www.pathologyinafrica.org/surveydata/map-data.php?type=n_path%7Cmin-max%7C1%7C1%7C1%7CNumber+of+Pathologists+Per+Million+Population#

3. ASSESSING HER2 EXPRESSION IN HUMAN BREAST CANCER CELLS

3.1 Introduction

Each year, around 230,000 people in the United States are diagnosed with invasive breast cancer[44]. Of these, approximately 15-20%, or 34,500-46,000, are found to overexpress the HER2 antigen and are classified as being HER2 positive (HER2+). As explained in Section 1.1, there is a clear need for a better biomarker to identify the presence of HER2 in immunohistochemistry (IHC), especially using MUSE on fresh biopsies. Our first proposed biomarker, titled CB11-CPN680, combines the CB11 primary anti-HER2 antibody [Abcam], the standard antibody used in HER2 IHC, with a custom polymer nanoparticle (CPN) [Stream Bio] that is UV-excitable and emits a bright red color (680 nm). CPN680 was chosen over other CPNs because it is the closest available color to the reddish-brown emission of traditional HER2 IHC stains. This biomarker should increase the sensitivity of CoreView-MUSE IHC because they are known to be 100-1000x brighter than Quantum Dots (Qdots), which are already significantly brighter than current stains used in IHC[45]. The CB11-CPN680 biomarker has a diameter of around 80 nm, which makes it too large to penetrate the plasma membrane, even with temporary membrane disruption with Triton X-100. As a result, CPNs will most likely be unavailable for use in intracellular staining of antigens such as ER and PR, but this has yet to be explored. Despite this, we are using CB11-CPN680 to confirm our theory that CoreView-MUSE can successfully perform HER2 IHC on fresh CNBs. If confirmed, we will adjust our protocols for smaller fluorescent molecules, such as Qdots, for ER and PR IHC.

3.2 BT-474 Cell Culture

The first step in evaluating the performance of the CB11-CPN680 biomarker is to confirm its ability to stain and identify the HER2 protein. To accomplish this, I am employing

the use of a HER2+/PR+/ER- human breast cancer cell line called BT-474 [ATCC]. To limit complexity and cost, a HER2- cell line is not used as a negative control. Instead, trastuzumab [Med Chem Express], described in Section 1.2, will be selectively applied to cell pellets immediately before staining with CB11-CPN680 to block a specified number of HER2 receptors. This should prevent CB11-CPN680 from binding and staining the trastuzumab-bound receptors, effectively lowering the IHC score of the sample. The growth medium used to culture the BT-474 cells is a solution of 450 mL of BenchStable™ DMEM (1X) + GlutaMAX™-I [gibco], 50 mL of 10% Fetal Bovine Serum (FBS) [gibco], and 5 mL of Penicillin Streptomycin [gibco]. Cells were cultured using BT-474-specific culturing techniques from ATCC[46] and Elabscience[47].

3.2.1 Handling of Cryopreserved Cells

Upon reception of the cryopreserved cells on dry ice, the cells were immediately thawed with rapid agitation in a 37ºC water bath for 60 seconds. After the wash, the vial was cleaned with 70% ethanol to ensure sterility. Next, the vial was opened, and the cells were transferred into a 15 ml Falcon centrifuge tube containing 9 mL of 37ºC growth medium. After combining the thawed cells and the growth medium, the solution was centrifuged at 500 rpm for 3 minutes in a Champion F-33D centrifuge [Ample Scientific]. After removing the supernatant, the cells were then resuspended in 10 mL of growth medium and transferred into a T75 vented-cap cell culture flask [Thermo Scientific] treated with 0.1% gelatin [Millipore] and placed in a 37ºC, 5% CO_2 dual stack incubator [3326, Forma Scientific].

3.2.2 Subculturing Protocols

Once the cells reached 70-80% confluence, assessed by eyesight and with a phase contrast inverted microscope [CK2, Olympus], they required subculturing with a 1:2 – 1:4 split ratio. If the cells had not reached this limit within 2 days of culture, the growth media was

replaced without removing the cells. To perform subculturing, first, the safety cabinet, centrifuge, and all materials were sprayed with 70% ethanol for disinfection. Next, the growth media was removed via pipetting and replaced with 3 mL of PBS [gibco] to remove all FBS. Next, the PBS was removed and 3 mL of 37ºC TrypLE Express [gibco] was added and incubated for 2-3 minutes to dissociate the adherent BT-474 cells from the surface of the T75 flask. To neutralize the TrypLE Express, 9 mL of growth media was added and then the entire solution of suspended cells was removed from the flask and split evenly between two 15 mL centrifuge tubes. Next, the solutions were centrifuged at 1000 rpm for 5 minutes and the supernatant was removed. Then, 10 mL of growth media was added to the tubes and then transferred into two T75 flasks for continued cell culture in the incubator. This protocol was intended to be performed indefinitely to produce cell pellets of approximately 10 million cells (~1.6 T75 flasks with 70-80% confluence) for MUSE IHC and standard histopathology.

3.2.3 Relevant Calculations

Basic calculations were performed in a Google Sheet (Appendix II) to estimate various numbers relevant to cell culture and staining. This Google Sheet is designed to take four inputs and display two outputs. The first input is the type of container and its number. This Google Sheet is designed to be used by future members of the Human Photonics Laboratory performing cell culture, so to make it more user-friendly, I made it available to take any common cell culture container. These include T flasks (T25, T75, T175, and T225), petri dishes (35, 60, 100, and 150 mm), and well plates (6, 12, 24, 48, and 96-well). Once selected, the sheet displays the seeding density, which is specific to each container, and the cells at 100% confluence and during subculture (75% confluence). The second input for the Google Sheet is which container is in use since the previous input can show all container types at once. This input is used to determine

approximately how many cells are present during subculture. The third input is how many containers are available for subculture. This input is used to calculate approximately how many total cells are present to determine if there are enough to test with the CB11-CPN680 biomarker. The final input is whether testing will be performed (YES/NO), which is used to determine how many cells are left for additional culturing and what the split ratio should be. The outputs of the Google Sheet are the split ratio and the number of containers needed to produce 10 million cells for MUSE imaging and standard histopathology. For my BT-474 cell culture with T75 flasks, it was determined that 6.3 million cells were available from each flask during subculture, so 1.6 flasks were needed to produce 10 million cells for testing. Furthermore, it was determined that a split ratio of 1:3 was needed for each flask not being used for testing.

3.2.4 Cell Culture Problems

Despite three separate attempts, I could not successfully culture the BT-474 cells for more than four weeks due to multiple problems. My first attempt at cell culture proved the best of three, with the cells thriving for weeks and producing more than enough live, healthy cells for analysis. Unfortunately, I was still waiting for shipment of the CB11-CPN680 biomarker and could not produce any MUSE images and results. Due to a stock-checking error on my part, there was not enough FBS to produce enough growth media to keep the exponentially growing cells alive, and they were starved as a result. My second attempt at culturing BT-474 cells lasted around two weeks before it proved unsuccessful. It was determined, using the inverted microscope, that these cells were killed by bacterial contamination, specifically mycoplasma. This was concluded by comparing the live imaging to online photos and videos, specifically how the particles moved and how they were most common around cells.

To prevent any contamination of the next cell culture attempt, I first attempted to identify the mechanism of contamination. To do this, I used 35 mm petri dishes [Fisher Scientific] to individually incubate each solution used during subculturing with and without growth media. These include the gelatin for treating the T75 flasks, the PBS used for rinsing out the growth media, the TrypLE Express used to disrupt adhesion, and the growth media. To assess bacterial contamination, I examined each petri dish before incubation, after 24 hours of incubation, and after 48 hours of incubation. At each time point, there was no sign of mycoplasma or any other contaminant in the petri dish. From these results, I concluded that the mycoplasma must have been introduced from myself, improper sterility techniques, and/or the broken biosafety cabinet in our lab. From this conclusion, the only solutions to prevent future contamination were to deep clean the incubator and biosafety cabinet and follow stricter sterility protocols. Unfortunately, these methods were not good enough, and the same mycoplasma bacterial contamination occurred in the third cell culture attempt. As a result, my attempts at culturing the BT-474 were forced to come to an end.

3.3 Plan for Staining, Imaging, and Diagnosis

3.3.1 Staining

Despite my inability to successfully produce 10+ million cells for MUSE imaging and analysis, I still had a thorough, well-researched plan for the staining, imaging, and subsequent diagnosis of the cell pellet. For staining, I adapted my protocols from cell pellet staining protocols available online on the National Institute of Environmental Health Sciences website[48]. First, BT-474 cells in around 1.6 T75 flasks of 70-80% confluence would be combined and centrifuged in two 15 mL centrifuge tubes at 500 rpm for 8 minutes. Then, the supernatant would be discarded, and the cells would be resuspended in Hank's Balanced Salt Solution (HBSS)

[Thermo Fisher Scientific], chilled to 4ºC in an ice water bath. Next, if a lower effective HER2 score is required, Trastuzumab would be added and incubated with the cells for 20 minutes in the ice bath. The amount of Trastuzumab depends on the desired HER2 IHC score (0-2+) and is determined using another Google Sheet. To make this calculation, I first had to estimate how many HER2 receptors should be bound by trastuzumab to properly reduce the amount of CB11-CPN680 binding. Previous studies have reported that the BT-474 cell line has around 2×10^6 HER2 receptors per cell[49-50]. Another study has shown that cancers diagnosed as HER2 0, 1+, 2+, and 3+ have approximately 2×10^4, 1×10^5, 5×10^5, and over 1×10^6 receptors per cell, respectively[51]. Therefore, to produce effective HER2 IHC scores of 0, 1+, and 2+ from BT-474 cells, enough trastuzumab must be added to block 1.98×10^{13}, 1.90×10^{13}, and 1.50×10^{13} receptors, respectively, in a pellet of approximately 10 million cells. Assuming one molecule of trastuzumab binds to one HER2 receptor, it should take 4.785, 4.592, and 3.625 µg of trastuzumab to reduce the HER2 IHC 3+ BT-474 cells to 0, 1+, and 2+, respectively. While this was theorized to work, it had never been tested before and was not tested in this study due to the cell culture problems identified in the previous section. After incubating the cells with trastuzumab, 2 mL of HBSS would be added, and the mixture would be centrifuged at 500 rpm for 6 minutes and then the supernatant would be discarded.

With or without trastuzumab to reduce the effective HER2 IHC score, the next step in the staining protocol is to add the CB11-CPN680 biomarker. This would be applied, according to the manufacturer, as a 200 µL solution of 10 µg/mL. After adding the CB11-CPN680, the antibody conjugate would be incubated with the cells in the 4ºC ice bath for 20 minutes. Next, 2 mL of HBSS would be added, the mixture would be centrifuged at 500 rpm for 6 minutes, and the

supernatant would be discarded. Lastly, the Hoechst nuclear stain and Rhodamine B cytoplasmic stain would be applied simultaneously in the same manner, but for 2 minutes instead of 20.

3.3.2 Imaging

After all staining is complete, the cell pellet would then be carefully transferred to a quartz coverslip [#72256-02, Electron Microscopy Sciences] (Figure 5a) for MUSE imaging. Quartz is chosen, over other materials such as sapphire and glass, as the coverslip for MUSE, because it has a refractive index (RI) of 1.49 at the 285 nm photons used by MUSE. This is lower, and thus more conductive of photons, then its counterparts, and offers the most intensely illuminated images and in-focus images. The difference in average nuclei focus quality between using a sapphire (1.82 RI) and a quartz coverslip was identified to be significant in my capstone project (Figure AIII.1). After transferring the stained cell pellet to the coverslip, the UV lights (Figure 5b) would be turned on, the ceiling lights would be turned off, and imaging would commence. For imaging, the MUSE system uses a 10x 0.3 NA objective lens [Plan Fluor, Nikon] (Figure 5c) attached to several Thorlabs optomechanical components and mirrors, leading the photons to a charge-coupled device (CCD) digital color camera [USB 3.0, Ximea] (Figure 5d). An objective lens positioning piezosystem [30V300CL, Piezosystem Jena] (Figure 4e) is used to manually control the plane of focus during imaging. This is used to produce 30-80 images of different focal planes to ensure that all cells are in complete focus. Images are taken and saved as TIFF files using the Ximea CamTool application, downloaded from the Ximea website. Imaging the entire surface of the cell pellet is enabled by two 1-axis motorized translational stages [MT1-Z8, Thorlabs] (Figure 5f), controlled by two brushed DC servo motor controllers [KDC101, Thorlabs] (Figure 5g), which are employed to control the x and y position of the coverslip. To combine all images at one positional frame into a single in-focus image, the

Helicon 7 application was used. This software renders a focus stack into a fully focused image by combining the sharpest areas of each image in the stack[52]. After all frames have been focused, Fiji ImageJ 2.0.0 is used to combine all images into a single stitched panorama. This is completed using the Grid/Collection Stitching plugin and the Sequential Images Type, which uses the Fourier Shift Theorem to yield cross-correlation measures to determine areas of best overlap[53]. Then, the plugin fuses the images and displays the result in an 8-bit image. To retain the colors, the fused image is then converted into a RGB Color image and saved as a TIFF file.

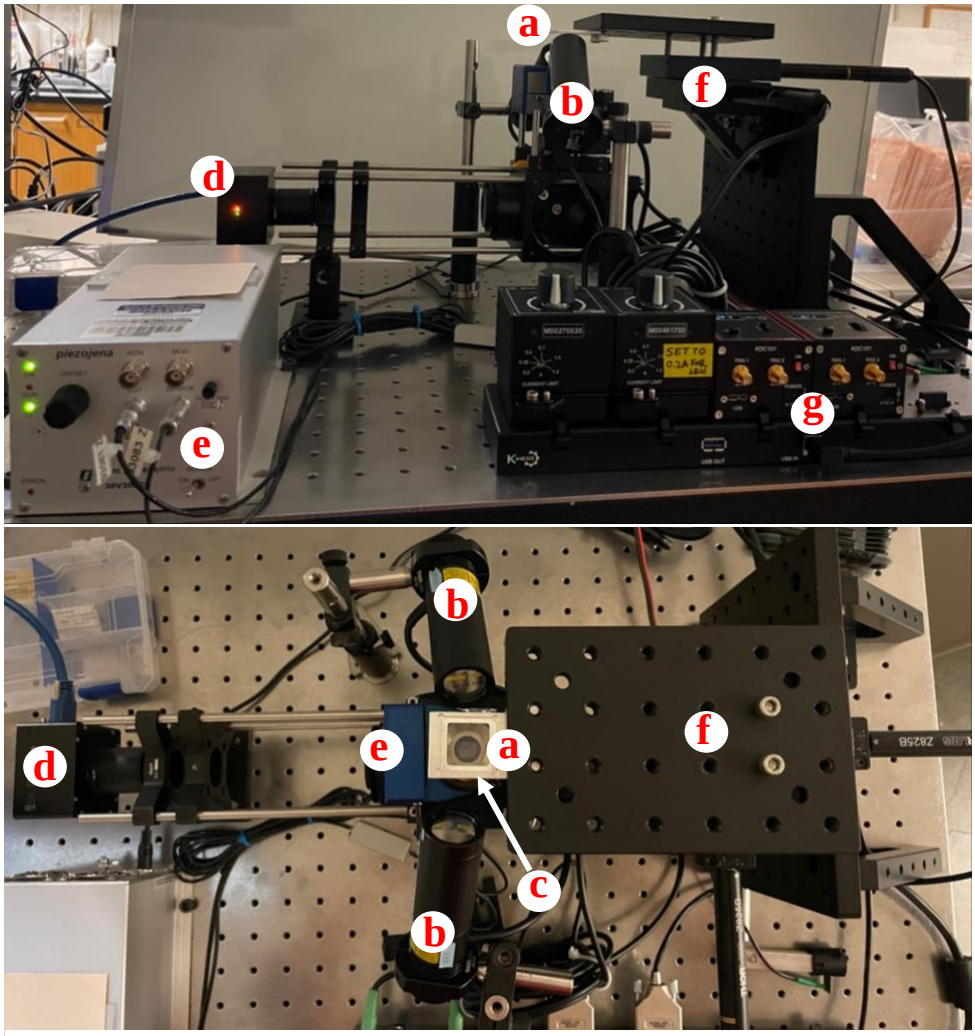

Figure 5 The MUSE imaging system hardware. The quartz coverslip (a) holds the biopsy above the 10X objective lens (c). The DUV LEDs (b) illuminate the sample for imaging via the color camera (d). A piezosystem (e) controls the plane-of-focus and two translational stages (f), controlled by motors (g) control the position of the coverslip over the lens.

3.3.3 Analysis and Diagnosis

To evaluate the effectiveness of the CB11-CPN680 biomarker at staining HER2 antigens, I would use three different metrics. The first, and fastest, metric would be performed using Fiji ImageJ to identify and count nuclei and CPNs. In this method, the stitched panorama is opened and then the scale is set to 1.6574 pixels/μm, as determined using a glass slide resolution target [USAF 1951, Edmund Optics]. Next, the RGB color image is split into Red, Green, and Blue channels. For my MUSE imaging, nuclei are present most intensely in the Blue channel and less intensely in the Green channel, with no presence in the Red channel. Therefore, to identify and count the number of stained nuclei, the Blue channel of the image is selected. The next step in the protocol is to subtract the background, which is performed using a rolling ball radius of 20.0 pixels and a dark background. After subtracting the background, a threshold is applied to identify and select the stained nuclei. In this thresholding, the default method is used with a limit of 15-255 on the image's histogram. After selecting the nuclei, they are counted using the Analyze Particles function with a size of 25 μm^2 – Infinity and a circularity of 0 – 1. 25 μm^2 is chosen as the lower limit for particle identification because the average mammalian cell nucleus has a diameter of 6 μm, giving an area of ~ 28 μm^2 [54]. The result is a list of each identified particle, its area, and its pixel value (255 for all after thresholding), but only the number of particles is recorded. Next, the number of CB11-CPN680s must be determined and displayed. This is performed using the same method employed to identify and count the nuclei in the image. However, because the CB11-CPN680 has an emission of 680 nm (red), it only appears in the Red channel, so this channel is used instead of Blue. Furthermore, because the biomarkers are more intense than Hoechst, the lower limit of the threshold is 20 instead of 15. Lastly, because the CB11-CPN680 antibody conjugate is approximately 70-80 nm in diameter, a lower limit of

3.5 is used when using the Analyze Particles function. The main difference between analyzing stained nuclei and the presence of CB11-CPN680 is what is recorded. Because the number of individually identified CB11-CPN680 biomarkers is of less diagnostic importance, 2 metrics are recorded. By selecting “Show: Overlay” when analyzing particles, the outline of each identified particle is shown over the thresholded image. Then, from this image, I manually count and record the number of cells with stained membranes as well as the rough percentage of the membrane that is stained on each cell. This is used, with the number of identified nuclei, to determine the percentage of cells that have any HER2 staining and the uniformity of membrane staining, which are both used to score HER2 IHC.

The second metric used to analyze and diagnose the HER2 staining of BT-474 cells with CB11-CPN680 is the formal diagnosis by Suzy Dintzis M.D. PhD, a breast cancer pathologist at UW Medicine. However, because pathologists are not trained to make a diagnosis from a MUSE image, it must first be transformed into standard H&E colors with a process called Virtual H&E. This process uses an application, titled “colormapper 05-20-16.exe”, that converts identified nuclei and identified background, by selecting one point of each one in the MUSE image, into the dark purple nuclei and pink background of H&E histopathology. To receive the clearest Virtual H&E image, the background must first be subtracted using a Pure Spectrum method. This is performed by setting the Gain of the Nuclei color channel to 0 and increasing the percentage of background subtracted until the white regions of the H&E image only contain nuclei. Next, the Threshold, Gain, and Gamma of the Background and Nuclei are adjusted until a desirable Virtual H&E image is produced. Virtual H&E images would then be sent to Dr. Dintzis to diagnose the HER2 IHC score. This diagnosis would then be compared to the third metric of evaluation: gold standard H&E and HER2 IHC histopathology. To produce these images, two

cell pellets, produced from 3 T75 flasks, would be sent to Brian Johnson and the Histology and Imaging Core (HIC) at the University of Washington. The first cell pellet would be the stained pellet used in MUSE imaging, to evaluate whether Hoechst, Rhodamine B, and CB11-CPN680 staining affect downstream histopathology. The second pellet would consist of the remaining, unstained, cells with or without trastuzumab incubation, depending on the intended IHC score. Although never tested, it was still unlikely that the trastuzumab-HER2 binding would survive the formalin fixation required to send the samples to the HIC. Therefore, the standard histopathology results for desired effective HER2 IHC 0, 1+, and 2+ would be unreliable. After imaging from the HIC, the images would be sent to Dr. Dintzis for professional diagnosis. For both Virtual H&E and standard histopathology diagnoses, the samples would be single-blinded, with Dr. Dintzis unaware of the intended IHC score and the predicted (with ImageJ) IHC score. The combined results of the predicted IHC score and Dr. Dintzis' diagnoses of the Virtual H&E and gold standard histopathology images would be used to confirm the ability of CB11-CPN680 to properly bind the HER2 antigen and stain with increased intensity.

3.4 References

44. Nitta H, Kelly D, Allred C, Jewell S, Peter B, Dennis E, Grogan TM. 2016. The assessment of HER2 status in breast cancer: the past, the present, and the future. *Pathology International*. 66, 313-324. DOI: 10.1111/pin.12407
45. CPN™ - Conjugated Polymer Nanoparticles. *Products & Services*. Stream Bio. Accessed April 4, 2021, from https://www.streambio.co.uk/our-technology/
46. BT-474. *Human Cells*. ATCC. Accessed July 28, 2021, from https://www.atcc.org/products/htb-20
47. BT-474 [BT474] Cell Line. *Elabscience*. Print.
48. Stockton P. 2003. Special Techniques Cell Pellet Protocol. *National Institute of Environmental Health Sciences*. National Institute of Health. Accessed July 29, 2021, from https://www.niehs.nih.gov/research/atniehs/labs/assets/docs/a_d/cell_pellet_protocol_508.pdf
49. Hathaway HJ, Butler KS, Adolphi NL, Lovato DM, Belfon R, Fegan D, Monson TC, Trujillo JE, Tessier TE, Bryant HC, Huber DL, Larson RS, Flynn ER. 2011. Detection of

breast cancer cells using targeted magnetic nanoparticles and ultra-sensitive magnetic field sensors. *Breast Cancer Research*. 13:5, R108. DOI: 10.1186/bcr3050
50. Onsum MD, Geretti E, Paragas V, Kudla AJ, Moulis SP, Luus L, Wickham TJ, McDonagh CF, MacBeath G, Hendriks BS. 2013. Single-Cell Quantitative HER2 Measurement Identifies Heterogeneity and Distinct Subgroups within Traditionally Defined HER2-Positive Patients. *The American Journal of Pathology*. 183:5, 1446-1460. DOI: 10.1016/j.ajpath.2013.07.015
51. Hendriks BS, Klinz SG, Reynolds JG, Espelin CW, Gaddy DF, Wickham TJ. 2013. Impact of Tumor HER2/ERBB2 Expression Level on HER2-Targeted Liposomal Doxorubicin-Mediated Drug Delivery: Multiple Low-Affinity Interactions Lead to a Threshold Effect. *Molecular Cancer Therapeutics*. 12:9, 1816-1828. DOI: 10.1158/1535-7163.MCT-13-0180
52. Helicon Focus Help. Accessed June 5, 2020, from https://www.heliconsoft.com/focus/help/english/HeliconFocus.html
53. Preibisch S. Grid/Collection Stitching Plugin. Accessed June 5, 2020, from https://imagej.net/Grid/Collection_Stitching_Plugin
54. Alberts B, Johnson A, Lewis J, Raff M, Roberts K, Walter P. 2002. *Molecular biology of the cell* (4th ed.). New York: Garland Science. p. 197. ISBN 978-0-8153-4702-0

4. ASSESSING HER2 EXPRESSION IN FRESH HUMAN BREAST SPECIMENS

4.1 Introduction

In designing my master's project akin to a clinical trial, the logical, and feasible, next step in evaluating the CB11-CPN680's performance is to use it to stain fresh human breast cancer specimens. This is even more important after the unsuccessful attempts of culturing cells described in Section 3.2.4. While FFPE sections of HER2+/- breast cancer are widely available, they do not meet the requirements of fresh tissue necessary to evaluate the performance of CoreView-MUSE, as previously described. Therefore, to properly assess the ability of CB11-CPN680, and future IHC biomarkers, to work in CoreView MUSE, we are receiving freshly resected CNBs and tumor sections, from consenting patients at UW Medicine, through NW Biospecimen.

4.2 NW Biospecimen Requirements

The approval process required to receive human samples through NW Biospecimen is stringent, to ensure no patient information is improperly used. For this process, I had to first self-determine and prove that this study is IRB exempt. I completed this using an Exempt Determinations Worksheet from the University of Washington Human Subjects Division (Document AIV.1). This research is IRB exempt because it meets the requirements of Category 4: "Secondary research uses of identifiable private information or identifiable biospecimens for which consent is not required," because no identifiable patient information is recorded or shared[55]. Because this research is IRB exempt, I did not need to seek IRB approval through the University of Washington and could proceed with the NW Biospecimen approval process. The second required document was the research proposal for my project. This proposal outlined my plan for the human samples as well as the need for my research (Document AIV.2).

The last document needed to complete the NW Biospecimen approval process is the Study Registration Form (Document AIV.3). This form documents all contact and funding information for the project and details the requirements for specimen acquisition. Of these requirements, the first is that the samples needed for this study are fresh tissues (surgery or biopsies). These are needed over fixed samples and stained slides to ensure CB11-CPN680 will work in CoreView-MUSE on fresh CNBs. The next requirements pertain to the general population producing the specimens. Because gender, age, and race/ethnicity have no known effect on HER2 status and overexpression, any gender, age, and race/ethnicity are accepted for my study. Furthermore, because HER2 status and overexpression is also independent of all other possible exclusion criteria, including pregnancy, treatment, or prior cancer history, none were included in the requirements. The last requirements detailed in the Study Registration Form pertain to the tissue samples. The samples provided through NW Biospecimen must be mammary tissue from the breast and must be larger than a 2 x 2 x 12 mm rectangular block. This size requirement exists because it is the size of a standard breast CNB. Additionally, there are time requirements to ensure the specimen remains fresh until imaging is complete. According to Nitta et al., HER2 IHC staining has been shown to be reduced by a cold ischemic time of 4 hours on ice or 2 hours at room temperature[12]. Using the requirements detailed in the Study Registration Form, NW Biospecimen will screen all upcoming breast biopsies and will seek consent from qualifying patients for my use of their tissue. For significant statistical analysis, I would prefer to acquire 15 samples of each HER2 IHC score (0-3+), but this does not seem feasible because most HER2+ tumors are not large enough to produce samples for both histopathology *and* research. Despite this, I will pursue all the samples I can receive.

4.3 Staining and MUSE Imaging Protocols

Very similar methods to those described in Section 3.3 are employed to stain and image the human breast cancer samples, with some minor exceptions. All samples are received in saline from a cooler but are closer to room temperature than frozen. Once I arrive at Fluke Hall, after transporting the samples from UW Medicine, the staining process is immediately begun to prevent excess ischemic time. The staining process currently consists of 4 steps. The first step is incubating the sample with 2 µg of the CB11-CPN680 biomarker for 15 minutes in a 1.5 mL Eppendorf tube in the refrigerator. After HER2 staining, the sample is then rinsed in a 1.5 mL Eppendorf tube of PBS for 1 minute to remove excess CB11-CPN680 that may inhibit Hoechst and Rhodamine B staining. The third step of the staining process is staining with 0.01 µg of the Hoechst nuclear stain and 0.02 µg of the Rhodamine B cytoplasmic stain, simultaneously, for 3 minutes in another 1.5 mL Eppendorf tube. Lastly, the sample is rinsed for a second and third time in PBS for 1 minute to prevent excess stain from producing artifacts during imaging. After imaging on the quartz slide in the MUSE system, the samples are placed in 10% formalin for fixation prior to delivery to the HIC. While this process does not rely on the use of trastuzumab to effectively decrease the HER2 IHC score, trastuzumab can still be deployed if enough HER2+ samples have been received, stained, imaged, and analyzed. However, as Summer term comes to an end, this is looking extremely unlikely.

Sample	Date	Type	HER2	Stained	Unstained
1	5/26/21	CNB		3	0
2	6/2/21	CNB	NEG	2	1
3	6/30/21	CNB	NEG	2	1
4	7/1/21	SR	NEG	1	1
5	7/8/21	SR	NEG	1	1
6	8/2/21	CNB	NEG	3	1

Table 3. Human breast cancer samples: identifiers and other relevant information. HER2 classification is provided by NW Biospecimen as a positive (POS), negative (NEG), or unknown (blank). All given identifiers are not provided in this table for patient confidentiality and because they are not relevant to this research. Abbreviations: CNB = core needle biopsy; SR = surgical resection.

Each consented case through NW Biospecimen produces around 2-5 CNBs or 2-3 chunks of a surgical resection. Of these samples, the majority are stained using the protocol described above and the rest are left unstained to serve as negative controls for the second main objective of this project: to determine whether the CoreView-MUSE-compatible stains will affect downstream histopathology performed after CoreView ROSE adequacy. Additionally, because it is unknown how my stains will affect the gold standard histopathology performed after MUSE imaging, controls are needed to ensure the most accurate diagnosis is made. After imaging, both the stained and unstained sample(s) are delivered to the HIC in a 1.5 mL Eppendorf tube with 10% formalin. At the HIC, the samples go through the remaining FFPE steps and are then stained with H&E and the CB11 antibody conjugated to their typical HER2 fluorophore.

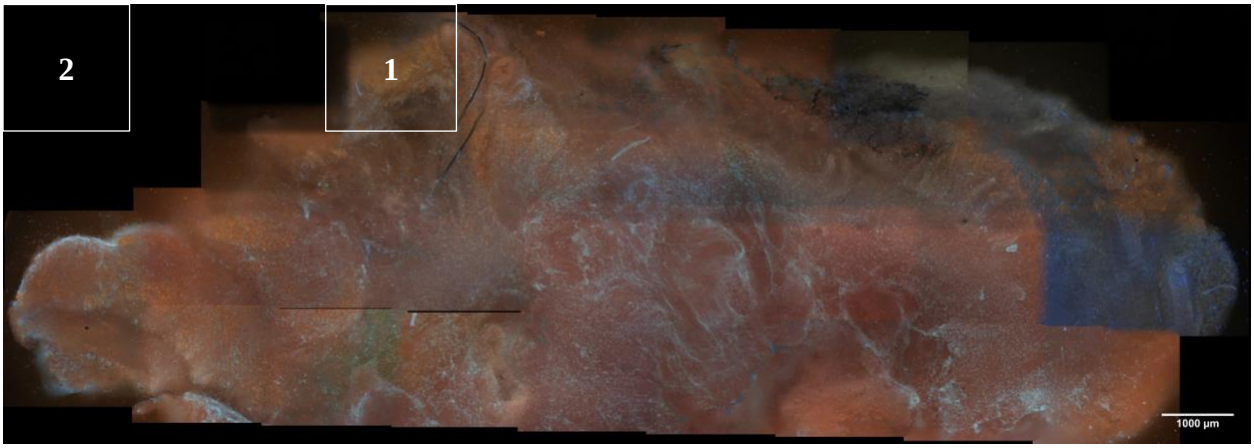

Figure 6 A stitched panorama of Sample 4.1 showing the likelihood of false corners. This image contains 40 individual MUSE images, including the blank frames needed to produce a rectangular grid, stitched into a single image in Fiji ImageJ. Square 1 was believed to be the upper-left corner of the specimen and was the first imaged. Square 2 is the true upper-left corner and is a blank image added after imaging was complete.

As stated, the methods used to image the human breast cancer samples are very similar to the methods that would have been used to image the cell pellets, detailed in Section 3.3. In fact, the only notable difference in imaging is that the fresh human samples have a larger surface area on the coverslip, so more frames are required to image the entire surface of the biopsy. Because there are many frames, between 20 and 30 for short CNBs and 40 and 100 for sections of

surgical resections, the Sequential Images type was found to be inaccurate at stitching the frames into a single panorama image. Instead, the “Grid: row-by-row” Type is used in the Grid/Collection stitching plugin. This type requires the images to include their numerical position in their filename, which is more difficult than it seems. When imaging the samples, I attempt to start at the top left corner of the specimen. However, it often proves to be a false corner under the MUSE microscope, and subsequent rows require more images than the first, etc. (Figure 6). As a result, I must add a blank MUSE image to fill in the gaps that prevent the current image from existing as a perfect rectangle. This is done by adding the same image, taken using MUSE and the quartz coverslip without tissue (Figure AIII.2) to the proper rows and columns of the grid of images. These additions frequently disrupt the numerical order of the images, forcing me to manually change the filename of each affected image. Luckily, this is of least concern for CNBs, which have more defined and uniform edges, so the stitching process should not require the addition of blank images when used in CoreView. With these outlined adaptations, all the imaging and image processing methods planned for the BT-474 cells were confirmed to work for this study during their use on the first human breast cancer sample, as I did not have a chance to test them on the cell line.

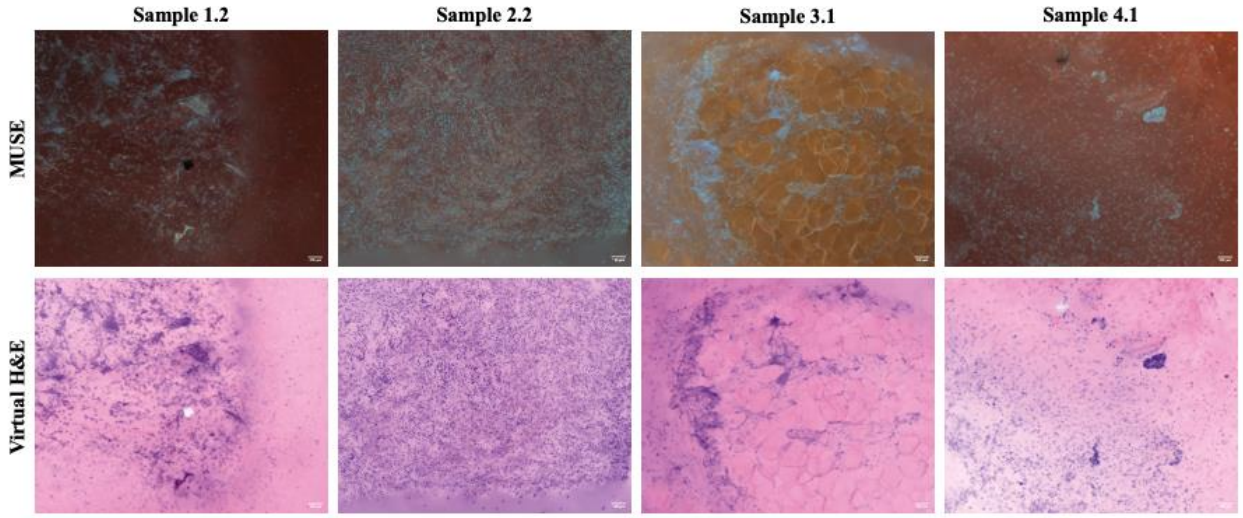

Figure 7 MUSE images of fresh human breast cancer and their Virtual H&E transformations. These images show that Hoechst (blue in MUSE, purple in Virtual H&E) and Rhodamine B (reddish yellow in MUSE, pink in Virtual H&E) can be successfully used with the colormapper application to produce images similar in color to H&E histopathology.

4.4 Imaging Results and Comparative Diagnoses

As of August 31, 2021, I have received samples from 6 patients. All relevant information regarding these samples, known at the time of collection and provided by NW Biospecimen, are included in Table 3. Due to human error, Sample 1 did not have an unstained specimen. All unstained biopsies are not imaged with the MUSE system and are immediately fixed in formalin for the HIC. A representative MUSE images and their Virtual H&E transformations of the first four imaged specimens can be seen in Figure 7. For clarification, Sample 4.2 is Sample 4.1 flipped over, and Sample 4.3 is the second section of the Sample 4 surgical resection.

Sample	Type	Frames	Pano?
1.1	CNB	4	NO
1.2	CNB	5	NO
2.1	CNB	8	NO
2.2	CNB	7	NO
3.1	CNB	21	YES
3.2	CNB	32	YES
4.1	SR	40	YES
4.2	SR	45	YES
5.1	SR	119	YES
6.1	CNB	39	YES
6.2	CNB	33	YES
6.3	CNB	33	YES

Table 4 A table showing the number of single frames for each sample and if a panorama was created.
Abbr: CNB = core needle biopsy
SR = surgical resection.

4.4.1 Results of the HER2 IHC Scoring Prediction Plugin

I have taken a total of 386 fully focused images of the 6 samples. The image spread and whether panoramas were made are shown in Table 4. The process of predicting the HER2 IHC score with Fiji ImageJ, detailed in Section 3.3.3, is shown for a single frame of Sample 1.1 in Figure 8. Results from this process for all samples and chosen single frames are presented in Tables 5 and AV, respectively.

Sample	CPN Cells	Nuclei	% Cells w/ CPN	Average Uniformity	HER2 Score/Status		
					Prediction	Diagnosis	Known
3.1	211	18455	1.14%	21%	0	0	NEG
3.2	174	27631	0.63%	40%	0	0	NEG
4.1	544	22210	2.45%	22%	0	0	NEG
4.2	671	21749	3.09%	22%	0	0	NEG
5.1*	1115	31217	3.57%	23%	0	0	NEG
6.1	240	38504	0.62%	14%	0	0	NEG
6.2	149	14912	1.00%	24%	0	0	NEG
6.3	100	15134	0.66%	15%	0	0	NEG

Table 5 Results of my HER2 scoring prediction plugin on MUSE panoramas. These results are compared to the known HER2 status of the specimen and the diagnosed HER2 score of the sample. *Sample 5.1 cannot be reliably analyzed due to the lack of cytoplasm staining.

Each analyzed MUSE panorama was predicted, using Table 1, to have a HER2 score of 0. This is because each sample has less than 5% of nucleated cells with detectable CPN680 staining and none have an intense (>75%) average membrane staining. These predictions agree with the previously known HER2 scores of the breast cancer specimens provided by NW Biospecimen. They also agree with the HER2 scores of the control samples after standard histopathology, diagnosed by Dr. Dintzis. These results show that my prediction plugin can accurately score MUSE images of fresh human breast cancer samples that are HER2-. I cannot ascertain its accuracy of scoring HER2+ samples until I have acquired and analyzed a HER2+ fresh breast cancer sample. In addition to the panoramas, I also analyzed chosen single frames and compared my prediction plugin's results to the known HER2 status of the specimen and Dr.

Dintzis' diagnosis of the same MUSE and Virtual H&E single frame images (Table AV). The results of these comparisons also show that my prediction plugin can accurately assess the HER2 score of a HER2- sample from its MUSE images. However, there are a couple single frames that were predicted to be 1+ or 2+ (Frames 4.2.30 and 4.2.44, Table AV), which still agree with the negative HER2 status. For these images, Dr. Dintzis was unable to provide a HER2 score (U), despite "apparent membrane staining", because there was limited nuclear and cytoplasmic detail. I will discuss the causes of this problem later, but this result shows that the 1+ and 2+ predictions may be correct. Lastly, I chose to not use Rhodamine B in the staining of Sample 5.1 because I was unsure of its effect on CPN680 detection by the prediction plugin because it emits a reddish-yellow color that also appears in the Red channel of the MUSE image. While I did not notice a difference in detected membrane staining, losing the cytoplasmic stain made it very difficult to identify cells in the MUSE and Virtual H&E images (Figure AV.1). This made it nearly impossible to assess the number of cells with CPN staining along with the uniformity of staining.

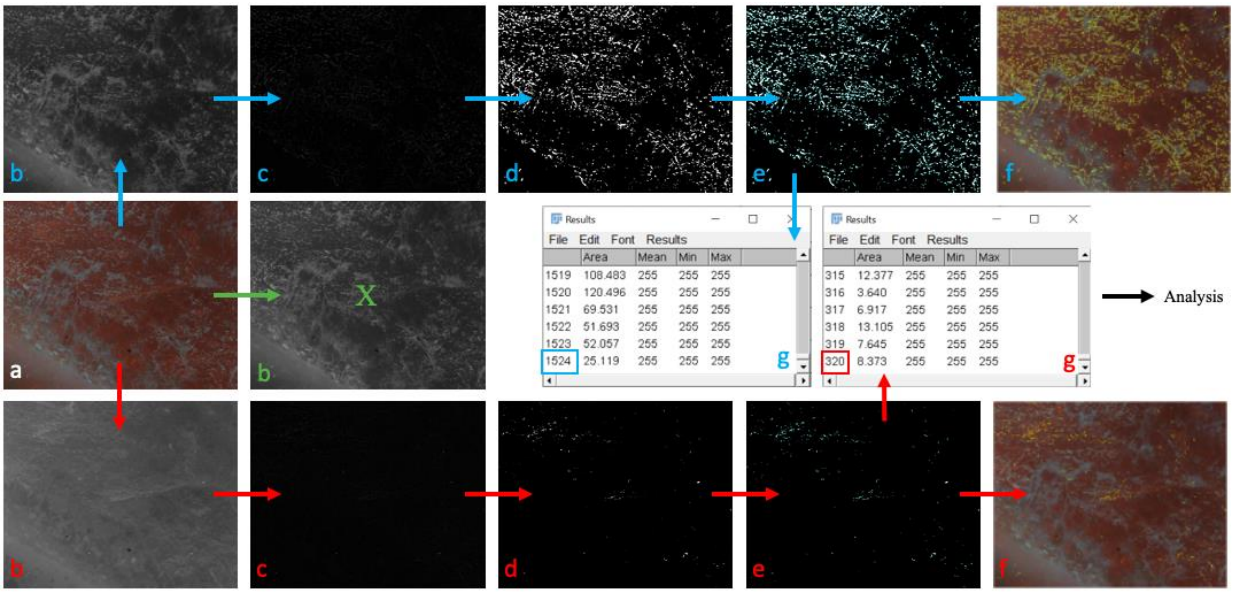

Figure 8 The predictive HER2 IHC score image processing performed in Fiji ImageJ on the first frame of Sample 1.1. First, the original image (a) is split into red, green, and blue color channels (b). Then the blue and red images have their background subtracted (c) and are thresholded (d). Lastly, a plugin is used to identify and count the number of nuclei and CPNs (e), with the results shown in (g). The identified nuclei and CPNs are overlayed over the original image for visual clarity (f).

4.4.2 Comparative Diagnostic Results

The second metric I am using to evaluate the effectiveness and accuracy of the CB11-CPN680 biomarker is a comparative diagnosis of a MUSE/Virtual H&E image and a gold standard histopathology image of the same sample, as described in Section 3.3.3. Through a Dropbox folder and an NDP.view link, Dr. Dintzis had access to all MUSE and Virtual H&E images, both single frames and panoramas, as well as all gold standard histopathology images received from the HIC. All MUSE/Virtual H&E images have scale bars added to the bottom right corner using Fiji ImageJ to aid in the diagnosis. Dr. Dintzis is blinded to all but the filenames of the images, which contain the sample number. She is unaware of the known HER2 status, provided by NW Biospecimen, the predicted HER2 IHC score, and any predictions made by the HIC, which were occasionally conveyed to me upon reception of the images.

Comparative diagnostic analysis for each able sample by Dr. Dintzis is provided in Figures 9-12 with full results in Figures AVI.1-2. A comparative diagnosis for Samples 5 and 6 could not be completed because the HIC has not finished the HER2 IHC on these samples. In summary, Dr. Dintzis was unable to render histologic evaluations of the fresh human breast cancer specimens using the MUSE and Virtual H&E images because they did not have clear nuclear and cytoplasmic details. Without these details, she could not diagnose the cancer type nor the HER2 IHC score when membrane staining was apparent. This problem is a result of the 10-20 microns of optical sectioning thickness of DUV light in our MUSE configuration. Fortunately, this can be remedied using a variety of techniques to manipulate the penetration distance of the DUV photons. One solution that has been previously studied relies on the immersion of the DUV LEDs in water[56]. This method relies on the refraction of light that occurs when the photons travel between the water and the coverslip to limit the penetration depth of the

DUV light. While this method was successfully shown to improve the nuclear and cytoplasmic details of MUSE images, it is not feasible for our MUSE setup because our camera and LEDs are beneath the tissue specimen (Figure 5). Another approach that could improve the quality and clarity of our MUSE images is using an objective lens with a higher numerical aperture (NA). Our current setup uses a 10x, 0.3 NA objective lens, which has a depth-of-field of 10 µm. By swapping our lens with a 20x, 1.0 NA objective (1.5 µm depth-of-field), we could limit the amount of background fluorescence that is imaged. Unfortunately, until we can successfully implement biopsy compression with the CoreView system, there is not enough tissue in the planes of focus to produce clear, fully focused, diagnosable images of fresh core needle biopsies with the decreased depth-of-field. This is evident by the approximately 10-20% of the surface in focus at a time using the 10x, 0.3 NA objective.

Lastly, a novel staining approach could be implemented to produce MUSE images with greater nuclear and cytoplasmic details. I theorize that a non-fluorescent DUV-absorbing molecule (dark quencher) could be used to reduce the amount of background fluorescence, limiting most noise behind the surface cells. To properly function, this molecule would need to be large enough to never penetrate the cell membrane to avoid blocking the imaging of cellular details. As a result, this molecule should only exist in the intercellular space. While this would prevent imaging of intercellular components, this should not impact a pathologist's diagnosis because most useful details are present on or within cells. The only major problem that could occur when using a DUV dark quencher with MUSE imaging is a decrease in staining intensity caused by the absorbance of DUV reflected horizontally at the surface of the specimen. Because most DUV light is reflected by unstained tissue, and the reflection occurs in random directions, staining absorption and subsequent intensity of visible fluorescence may be increased by

reflected DUV light. My theorized molecule would prevent this from occurring between cells, so stain intensity comparisons would need to be made between samples stained with and without the molecule.

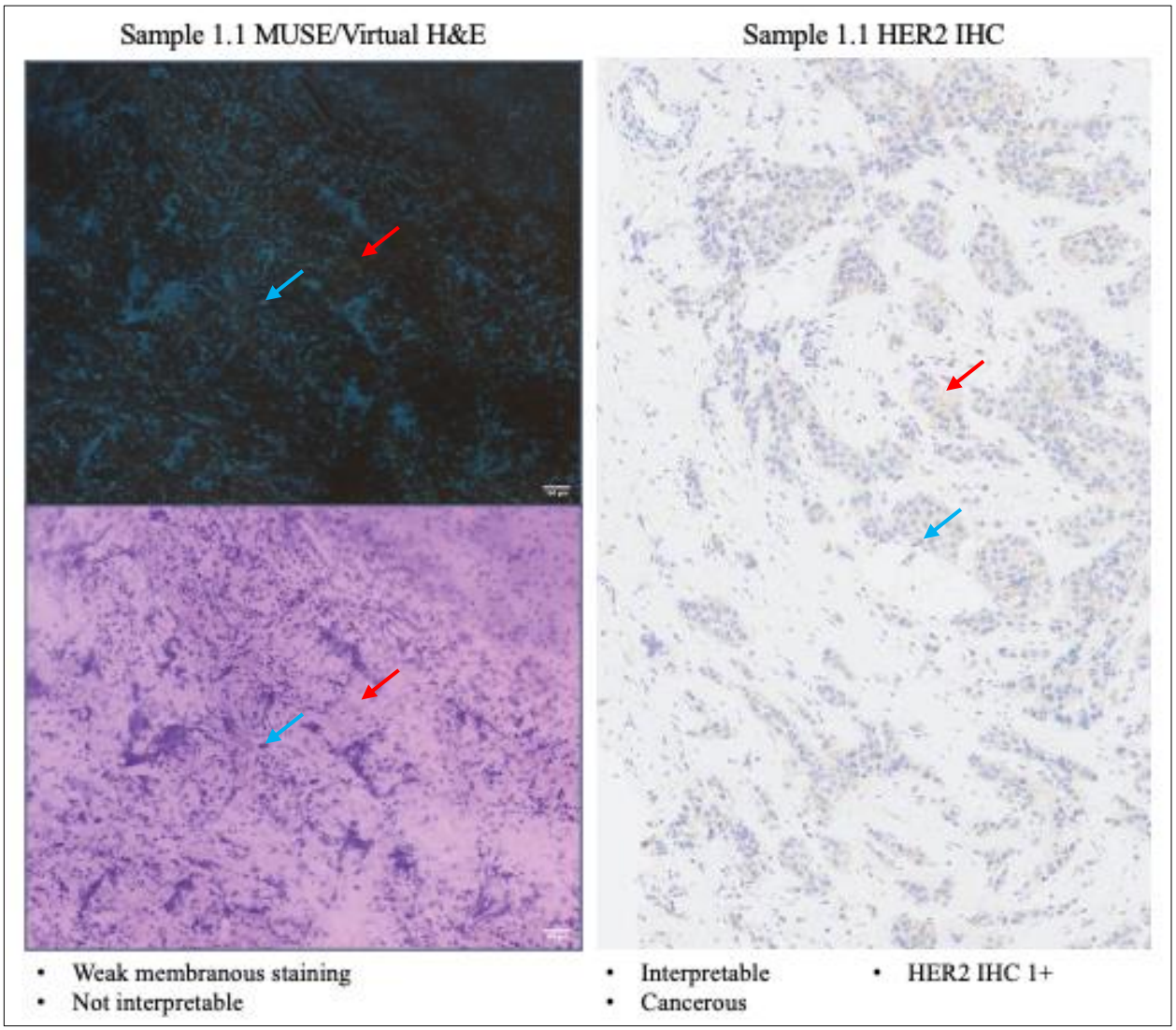

Figure 9 Comparative diagnosis of Sample 1.1. The MUSE and Virtual H&E images of Sample 1.1.2 have apparent weak membrane staining but was not interpretable. The HER2 IHC image of Sample 1.1 is interpretable, is cancerous, and is HER2 IHC 1+. Blue arrows identify one nuclei and red arrows identify one area of membrane staining per image.

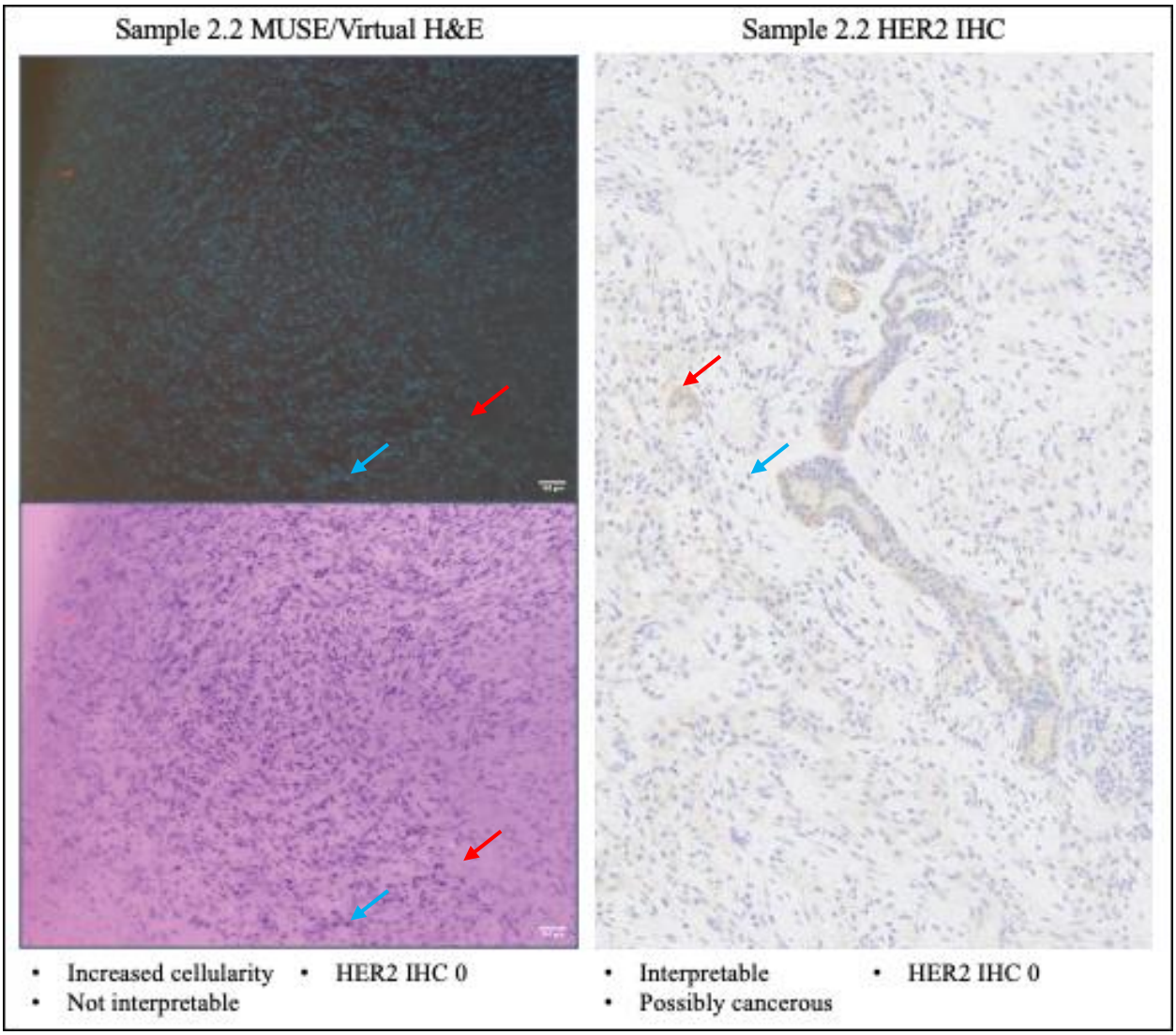

Figure 10 Comparative diagnosis of Sample 2.2. The MUSE and Virtual H&E images of Sample 2.2.6 have increased cellularity but are still not interpretable. The lack of membrane staining makes it easy to diagnose as HER2 IHC 0, however. The HER2 IHC image of Sample 2.2 is interpretable, is possibly cancerous (fibroinflammatory or spindle cell carcinoma but needs different staining), and is HER2 IHC 0. Blue arrows identify one nuclei and red arrows identify one area of membrane staining per image.

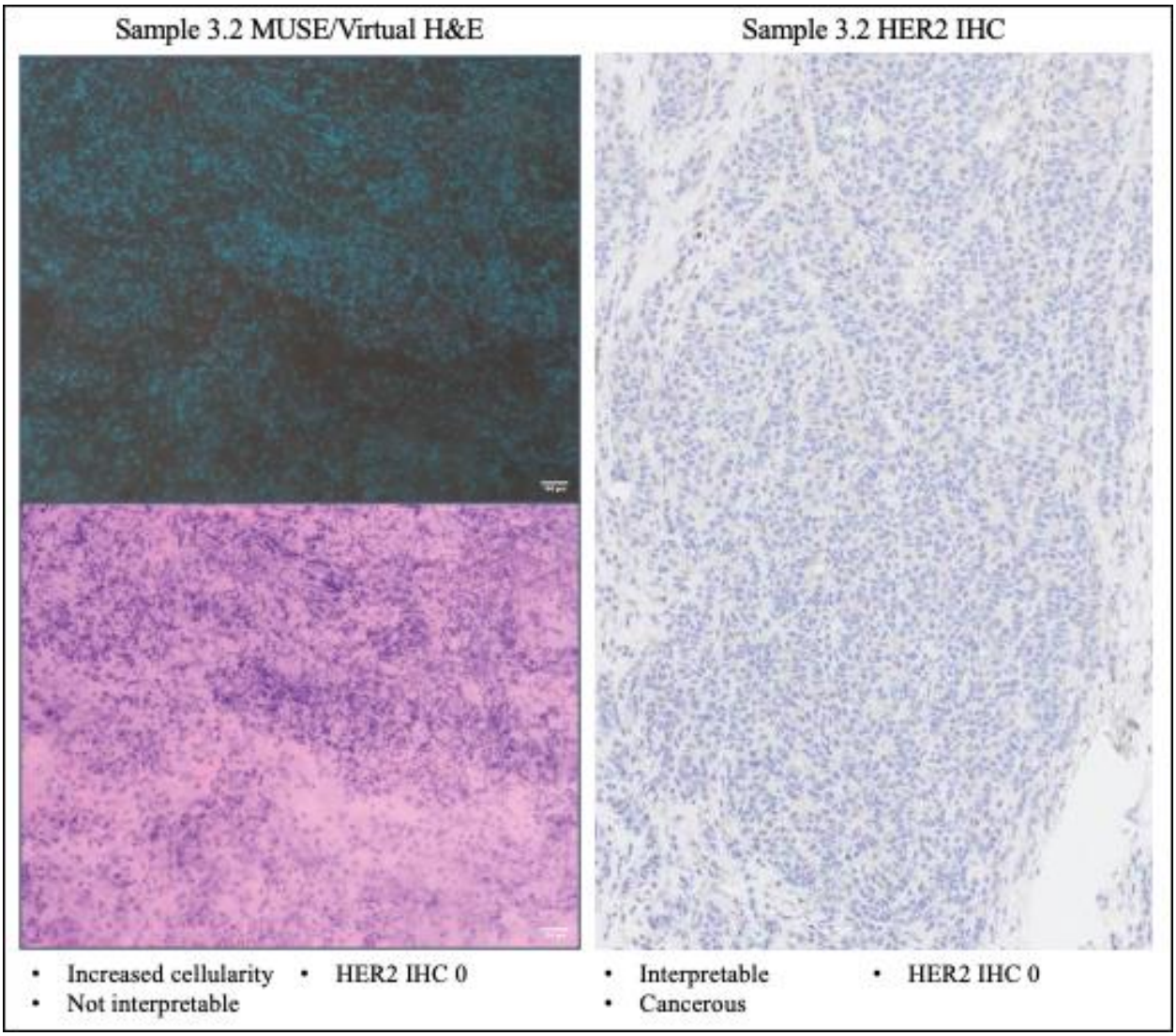

Figure 11 Comparative diagnosis of Sample 3.2. The MUSE and Virtual H&E images of Sample 3.2.12 have increased cellularity but are still not interpretable. The lack of membrane staining makes it easy to diagnose as HER2 IHC 0, however. The HER2 IHC image of Sample 3.2 is interpretable, is cancerous, and is HER2 IHC 0.

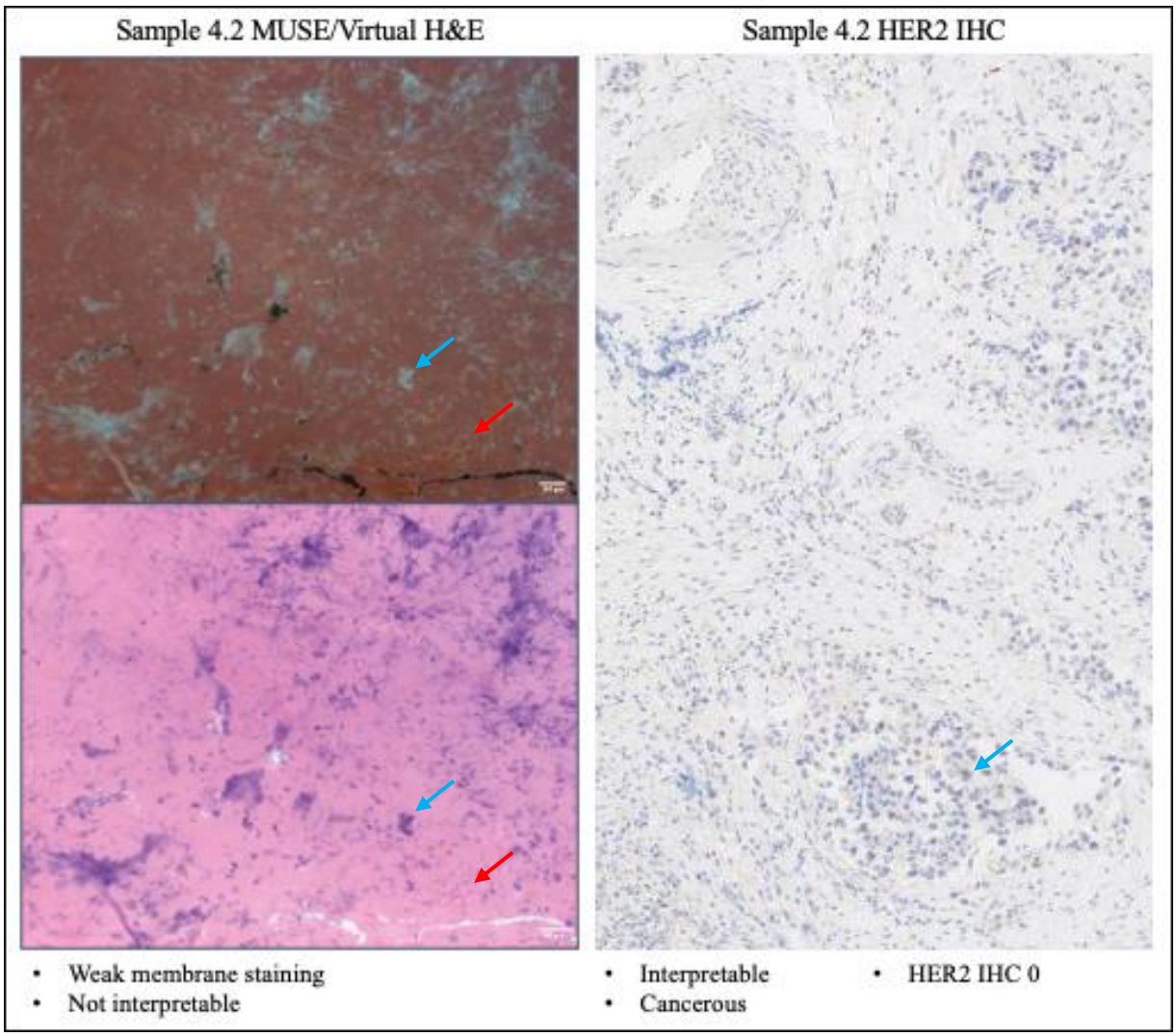

Figure 12 Comparative diagnosis of Sample 4.2. The MUSE and Virtual H&E images of Sample 4.2.30 have apparent weak membrane staining but was not interpretable. The HER2 IHC image of Sample 4.2 is interpretable, is cancerous, and is HER2 IHC 0. Blue arrows identify one nuclei and red arrows identify one area of membrane staining per image.

4.4.3 Assessing the Effects of Adequacy Stains on Downstream Histopathology

The second goal of my master's thesis is to assess the effects of the stains used in CoreView-MUSE adequacy on downstream histopathology. Currently, our adequacy stains consist of Hoechst and Rhodamine B (H&RB), but they may include CB11-CPN680 and other special stains later. To determine if staining with H&RB and CB11-CPN680 for MUSE imaging affects downstream histopathology, I am directly comparing the staining in H&E histopathology and HER2 IHC images of stained and unstained slides from fresh human breast cancer

specimens from the same patient. For a more professional conclusion, I am also comparing Dr. Dintzis' previous diagnosis of the samples. This evaluation was for the comparative diagnoses in Section 4.4.2, and she was unaware the HIC images had been stained prior to standard histopathology.

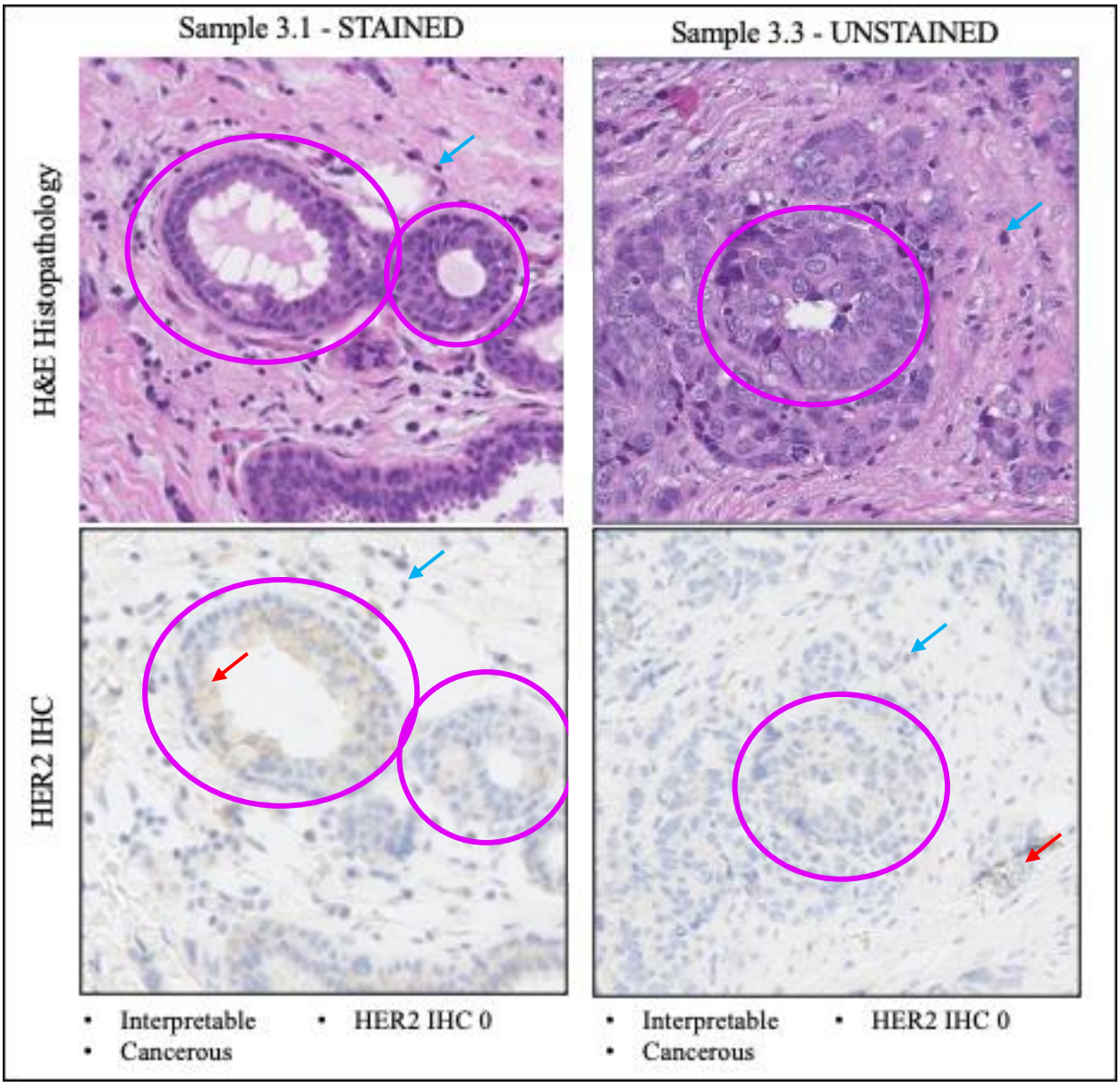

Figure 13 Standard histopathology adequacy staining comparison of Sample 3. Both the stained and unstained samples are interpretable and cancerous and have the same diagnosed HER2 IHC score. Furthermore, there is no apparent difference in nuclei, cytoplasm, nor membrane staining between samples. Pink circles identify milk ducts, blue arrows identify nuclei, and red arrows identify HER2 staining.

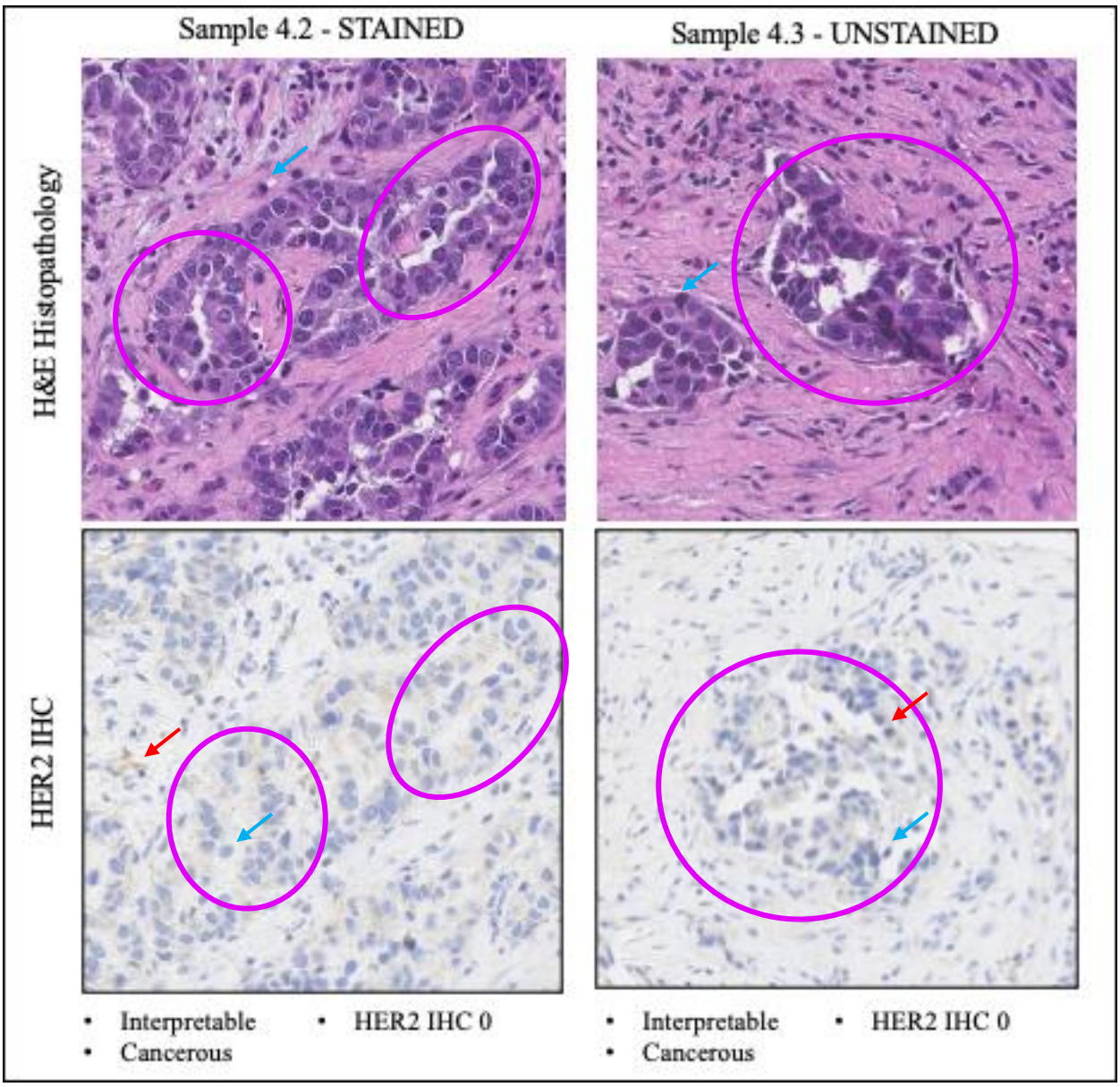

Figure 14 Standard histopathology adequacy staining comparison of Sample 4. Both the stained and unstained samples are interpretable and cancerous and have the same diagnosed HER2 IHC score. Furthermore, there is no apparent difference in nuclei, cytoplasm, nor membrane staining between samples. Pink circles identify milk ducts, blue arrows identify nuclei, and red arrows identify HER2 staining.

The results of this analysis are presented in Figures 13-14, and Dr. Dintzis' diagnoses can be seen in Figure AVI.2. Samples 3 and 4 were chosen for this analysis because they had unstained controls (Table 3) and have been imaged by the HIC. Sample 2 was not chosen

because although it was interpretable, Dr. Dintzis was unable to diagnose the sample as cancerous without further staining unrelated to my study. These results show that the stains used to perform adequacy tests in the CoreView-MUSE system do not disrupt downstream histopathology because there is no qualitative difference in H&E and HER2 IHC staining, and both samples were interpretable by Dr. Dintzis.

4.5 Adapting to Circumstances

I have encountered many challenges and setbacks throughout my work on this master's thesis. Firstly, the departmental guidelines after the onset of the COVID-19 pandemic barred me from starting my in-person research in the Summer 2020 term, which was my original intention. While this gave me time to perform an in-depth literature search and review, it produced an ordering of materials setback that was not overcome until halfway through the Autumn 2020 term. Despite this setback, I was on track to finish the analysis of the BT-474 cell culture and imaging. Unfortunately, as previously described, this did not succeed. Lastly, the application process for the NW Biospecimen human breast cancer samples was longer than I expected, and the samples come infrequently. This has resulted in the reception of only 6 samples as of August 31, 2021. Furthermore, none of the samples have contained HER2+ breast cancer, so I do not have a positive control sample to aid Dr. Dintzis in her diagnoses.

4.5.1 FFPE Control Slides

To adapt to this setback, I employed the use of 6 FFPE breast cancer tissue slides from AMS Biotechnology[57]. Of these samples, 3 are HER2+ and 3 are HER2- cancers. While not fresh tissue, and thus not fully representative of the use of CB11-CPN680 in CoreView, the FFPE slides can still be used to confirm the specificity and sensitivity of the biomarker in MUSE. My plan for these 6 samples was to stain 1 slide of each HER2 status with CB11-

CPN680 and Hoechst/Rhodamine B and image them with the MUSE system. For successful staining of these FFPE slides, antigen retrieval must be performed, as discussed in Section 1.1. To perform antigen retrieval, I followed the protocol used by Migliozzi and colleagues, who also used FFPE slides from AMS Biotechnology[58]. I also included methods from different sources found on the web. My antigen retrieval protocol used a 95ºC citrate buffer bath on a hot plate with overlapping slides for 15 minutes (Appendix VII)[59-60]. After successful staining and imaging, the slides were sent to the HIC for gold standard histopathology. My plan for the other FFPE slides is for them to serve as positive and negative controls. One slide of HER2+ and one slide of HER2- breast cancer will be sent directly to the HIC, without staining or deparaffination, to serve as a positive and negative control, respectively, for the gold standard histopathology images of the NW Biospecimen human specimens. The remaining two slides will serve as negative controls as they will only be stained with Hoechst and Rhodamine B (no CB11-CPN680) following deparaffination and antigen retrieval.

The results of the MUSE imaging and standard HER2 IHC of the FFPE slides are shown in Figures 15 and 16. The displayed images were chosen over others because they contain milk ducts, and the slides are known to have ductal carcinoma. As evident in the figures, there is a clear difference in color and intensity when the CB11-CPN680 HER2 biomarker is used to stain the HER2+ slide, compared to the HER2+ slide not stained with the biomarker and the HER2- MUSE images. This suggests that there is additional staining present in the HER2+ positive control slide that does not exist in the HER2+ negative control slide, etc. This is supported by Dr. Dintzis' qualitative analysis of the MUSE/Virtual H&E images, in which she concluded there is "apparent membrane staining" only in the HER2+ slide stained with CB11-CPN680. Dr. Dintzis was also able to interpret the MUSE/Virtual H&E images and diagnose them as

cancerous, which she was unable to do with the images of whole fresh core needle biopsies, as described in Section 4.4.2. This shows that MUSE *can* be used to produce diagnostic-quality images using our CoreView adequacy stains if the optical sectioning thickness can be limited. Oddly, there was no Hoechst nuclear staining in the HER2- FFPE slides despite identical deparaffination and rehydration protocols and staining quantities and times. For the future use of FFPE slides with MUSE, DAPI should be tried, as it is a DUV-compatible blue nuclear stain that can only stain formalin fixed cells.

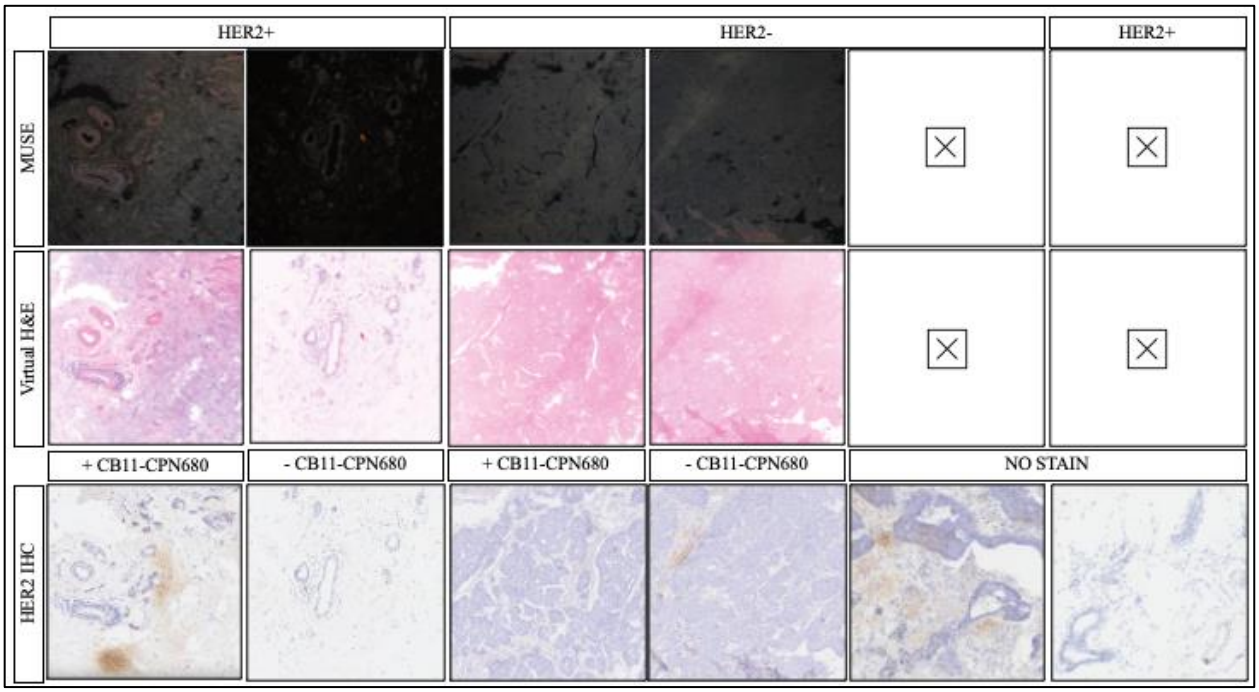

Figure 15 MUSE and standard HER2 IHC images of the FFPE control slides with different HER2 staining. Each sample is given its own column, with MUSE as the first row, the corresponding Virtual H&E image in the second row, and the HER2 IHC image in the third row. This comparison reveals a clear difference between MUSE/Virtual H&E images when the CB11-CPN680 HER2 biomarker is added to a HER2+ slide. IHC imaging provides less distinctive results. The "NO STAIN" columns do not have MUSE/Virtual H&E images as they were meant to serve as IHC controls. All images have 10x magnification.

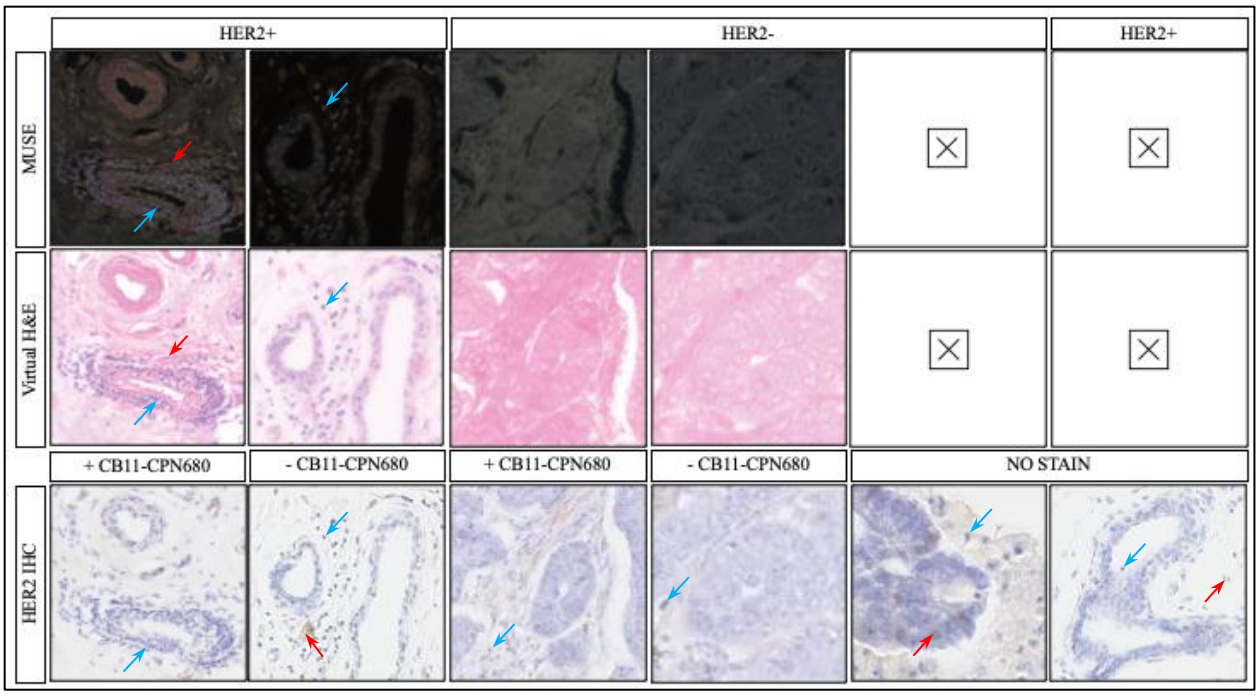

Figure 16 MUSE and standard HER2 IHC images of the FFPE control slides zoomed in to show details. Each image is from Figure 15 and is zoomed in on a potential milk duct (~20x). This qualitative comparison shows the clear difference in MUSE imaging when CB11-CPN680 is added to a HER2+ slide. It also shows the limited HER2 membrane staining in the IHC image of each slide. The "NO STAIN" columns do not have MUSE/Virtual H&E images as they were meant to serve as IHC controls. Blue arrows identify nuclei and red arrows identify HER2 staining.

While the FFPE slides provide decent evidence that CB11-CPN680 biomarker can be used to stain the HER2 antigen in the CoreView-MUSE system, the standard HER2 IHC performed by the HIC may not support this conclusion. As seen in Figures 15 and 16, there is little-to-no membrane staining in most of the HER2+ and HER2- FFPE slides, and all were given a HER2 score of 0 by Dr. Dintzis. Curiously, the majority of IHC staining (brown) that exists in intracellular, which should not occur with a HER2 marker. Due to this observation, and the previous MUSE imaging, I have concluded that the HIC imaging of the FFPE slides may not be reliable. There are several reasons this may have occurred. First, proper antigen retrieval may not have been conducted. I performed deparaffination, rehydration, and antigen retrieval on only the stained FFPE slides and left the control slides untouched. While I clearly stated this in writing and separated the stained and unstained slides, the HIC may not have used antigen retrieval on

the unstained slides. Due to the clear nuclear staining (blue) in the HER2 IHC images in Figures 15 and 16, it is very unlikely that the deparaffination and rehydration step was forgotten, so hopefully the antigen retrieval step was also performed. Second, the antibody used to stain the HER2 antigen may not be adequate. As the HIC is employing the CB11 antibody in these HER2 IHC protocols, hopefully this is not the case. While the CB11-CPN680-stained HER2+ FFPE slide provides some evidence that the CB11 antibody stains HER2, this cannot be fully concluded until a fresh HER2+ breast cancer specimen has been received from NW Biospecimen. Lastly, the FFPE slides may have been incorrectly cataloged and/or shipped by AMS Bio. Although the slides are confirmed, by Dr. Dintzis, to contain breast cells, they may not have the correct HER2 status. Unfortunately, there is no way to evaluate this possibility before the end of my thesis project.

4.6 References

55. WORKSHEET Exempt Determinations. Version #1.20, September 9, 2020. University of Washington Human Subjects Division.
56. Yoshitake T, Giacomelli MG, Quintana LM, Vardeh H, Cahill LC, Faulkner-Jones BE, Connolly JL, Do D, Fujimoto JG. 2018. Rapid histopathological imaging of skin and breast cancer surgical specimens using immersion microscopy with ultraviolet surface excitation. *Scientific Reports*. 8, 4476. DOI: 10.1038/s41598-018-22264-2
57. Tissues. *Biorepository*. Amsbio. Accessed August 1, 2021, from https://www.amsbio.com/products/biorepository/tissues
58. Migliozzi D, Nguyen HT, Gijs MAM. 2019. Combining fluorescence-based image segmentation and automated microfluidics for ultrafast cell-by-cell assessment of biomarkers for HER2-type breast carcinoma. *Journal of Biomedical Optics*. 24:2, 021204-1-021204-8. DOI: 10.1117/I.JBO.24.2.021204
59. Vinod KR, Jones D, Udupa V. 2016. A simple and effective heat induced antigen retrieval method. *MethodsX*. 3, 315-319. DOI: 10.1016/j.mex.2016.04.001
60. IHC antigen retrieval protocol. Abcam. Accessed August 31, 2021, from https://www.abcam.com/protocols/ihc-antigen-retrieval-protocol

5. SUMMARY AND CONCLUSIONS

In this thesis, I have introduced histopathology and the problems associated with it, including the time and labor required to prepare samples and the effectiveness of IHC stains. I have also introduced CoreView, our group's novel millifluidic device intended to replace much of the histopathology workflow. For CoreView to assess the immunophenotype of certain cancers, antibody conjugate stains that can work with fresh cells and have DUV/VIS excitation/emission must be developed. In this study, I have tested the specificity and sensitivity of CB11-CPN680, a novel HER2 biomarker that could be used to diagnose HER2+ breast cancer, one of the worst subtypes of invasive ductal carcinoma. Despite many challenges and setbacks, I have weakly concluded, using results from fresh tissue analysis and FFPE slides, that CB11-CPN680 can be used to stain the HER2 antigen in human breast cancer specimens for imaging with the CoreView-MUSE system. I cannot form a strong conclusion until HER2+ fresh human breast cancer samples have been received from consenting patients through NW Biospecimen, and imaged. The work conducted for my master's thesis has, however, shown that a fresh-tissue-compatible fluorescent molecule that excites under DUV illumination and emits wavelengths in the visible spectrum can be used to stain certain cancer markers. Previous studies have evaluated Qdots in MUSE with fixed tissue or in confocal microscopy with fresh tissue, but no immunophenotyping stain has been studied in fresh tissue imaging via MUSE. Despite the lack of fresh HER2+ breast cancer specimens, CB11-CPN680 membrane staining *was* seen in some HER2- samples that are likely HER2 IHC 1+ or 2+ (Figures 9, 12, AVI.1), showing that the biomarker can likely mark the HER2 antigen for MUSE imaging.

In addition to evaluating the effectiveness of the CB11-CPN680 HER2 biomarker when used in MUSE, I also assessed the effects of the CoreView adequacy stains on downstream

histopathology. These stains include the Hoechst nuclear stain, the Rhodamine B cytoplasmic stain, and the CB11-CPN680 HER2 biomarker, as a representative of all immunophenotyping stains, and the downstream tests include H&E histopathology and HER2 IHC. With a qualitative comparison of staining intensity (Figures 13-14) and comparative diagnoses (Figure AVI.2), it was concluded that the CoreView adequacy stains do not affect the ability of histopathology dyes to stain samples that have been fixed after CoreView-MUSE imaging. With this result, CoreView is able to function as an adequacy test at the point-of-care without preventing a full diagnosis from being made. However, future work is needed to produce interpretable MUSE images of whole fresh CNBs for successful CoreView operation.

APPENDICES

Appendix I – CoreView Biopsy Removal Data

Figure AI.1 Description of biopsy removal integrated chip experiment

Description: Biopsy removal experiments using TestChipV11_strippeddownforpottingbothsides.STL (Main_Chip_V11) - see figure
CNB gun is inserted into the cartridge and Hi Pressure Flow PBS is used to remove the exposed, 90deg rotated, CNB
The pressure of the flow begins at 2 psi and is raised by 2 psi until the biopsy is removed or the pressure reaches 10 psi
The PBS is flowed for 5 pulses, 3 times for each pressure, unless removed
Intactness of the CNB is determined via human judgement and is recorded at the CNB unsheathing and at each pressure
Each tissue was collected on 3/31/21 at 4:30PM and warmed in a 37•C water bath before experiments
CNB gun: Bard Mission 14g x 10cm; 10 cm penetration depth

Figure AI.2 Results of the integrated chip experiments

Table A2. Biopsy removal efficiency in the millifluidic cartridge - FULL RESULTS.

Tissue	Total	Start Intact		Finish Intact		Removal Pressure (psi)			Hours Since Resection
		N	%	N	%	Mean	Median	Std. Dev.	
Breast	20	20	100%	18	90%	3.50	3.0	1.933	1.33
Kidney	20	20	100%	20	100%	2.40	2.0	0.821	3.37
Lung	20	20	100%	19	95%	3.10	3.0	1.210	5.20
Pancreas	20	18	90%	17	85%	3.50	2.0	2.328	4.50
Total Kidney (w/ gauge exps)	30	30	100%	29	96.7%	2.8	2.0	1.45	

Table 3. Biopsy removal efficiency in the millifluidic cartridge.

Tissue	Removed from Needle	Biopsy Stayed Intact	Removal Pressure (psi)		
			Mean	Median	Std. Dev.
Breast	100%	90%	3.50	3.0	1.933
Kidney	100%	100%	2.40	2.0	0.821
Lung	100%	95%	3.10	3.0	1.210
Pancreas	100%	94%	3.50	2.0	2.328

Results from repeated core needle biopsy removal in the integrated millifluidic cartridge using fresh porcine breast, lung, kidney, and pancreas biopsies (n=20 of each). Biopsies are successfully removed if they are intact and removed from the needle within a pressure-driven flow of 10 psi.

Figure AI.3 Results of the proof-of-concept device

Table A1. Biopsy removal efficiency in the concept module - FULL RESULTS.

Tissue	Freshness	Total	Finish Intact		Released		Removal Pressure* (psi)		
			N	%	N	%	Mean	Median	Std. Dev.
Breast	Fresh	23	20	87%	20	87%	7.68	2.0	7.943
Breast	Refrigerated	6	2	33%	6	100%	4.83	5.0	2.927
Kidney	Fresh	21	16	76%	21	100%	3.38	2.0	5.035
Liver	Fresh	40	27	68%	39	98%	4.00	2.0	4.114
Lung	Refrigerated	25	24	96%	21	84%	9.00	10.0	7.826
Lymph Node	Fresh	5	3	60%	5	100%	6.80	5.0	5.630
Lymph Node	Refrigerated	26	21	81%	25	96%	3.96	2.0	3.233

Tissue	N	Removed from Needle	Biopsy Stayed Intact	Removal Pressure (psi)		
				Mean	Median	Std. Dev.
Breast	29	89.66%	75.86%	7.07	3.5	7.216
Kidney	21	100.00%	76.19%	3.38	2.0	5.035
Liver	40	97.50%	67.50%	4.00	2.0	4.114
Lung	25	84.00%	96.00%	9.00	10.0	7.826
Lymph Node	31	96.77%	77.42%	4.43	2.0	3.770

Results from repeated core needle biopsy removal in the biopsy removal concept module using porcine tissues of various organs and freshness. Biopsies are successfully removed if they are intact and removed from the needle within a pressure-driven flow of 25 psi.

* If the biopsy does not stay intact, removal pressure is recorded when the first section is released from the needle.

Table 1. Comparing needle orientation in the biopsy removal module.

Orientatation	N	Removed from Needle	Biopsy Stayed Intact	Removal Pressure* (psi)		
				Mean	Median	Std. Dev.
0°	20	100%	65.00%	15.15	17.50	8.586
90°	21	100%	76.19%	3.38	2.00	5.035

Results from comparing the orientation of the needle (degrees rotated from a top/superior unsheathing in the module). All CNBs were resected from the same fresh porcine kidney specimen. These results show that a 90º rotation results in more intact biopsies and requires much less pressure (volumetric flow rate) than biopsy removal with no rotation.

Figure AI.4 Porcine breast CNB data

Tissue:	Pig Breast
Fresh date:	4/2/21
Fresh time:	4:30 PM
Exp. date:	4/2/21
Exp. start time:	5:20 PM
Exp. end time:	6:20 PM
Time since fresh:	1:20
Exp. time:	1:00
NEEDLE:	Bard MaxCore
	14 gauge
	22 mm

Run	*P (psi)*	*Intact?*	*Removed?*	*Notes*
1	x	Y	x	unsheathed, intact but stringy and separated chunks
	2	Y	Y	took 1x pulses
2	x	Y	x	unsheathed, intact but stringy, in chunks, and visibly heterogeneous
	2	Y	Y	took 2x pulses
3	x	Y	x	unsheathed
	2	Y	Y	took 1x pulses
4	x	Y	x	unsheathed, peeled back, heterog.
	2	Y	Y	took 1x pulses
5	x	Y	x	unsheathed, stringy in chunks
	2	Y	Y	took 1 pulse
6	x	Y	x	unsheathed
	2	Y	N	stuck at back
	4	Y	N	stuck at back
	6	Y	Y	took 2x pulses
7	x	Y	x	unsheathed, peeled back
	2	Y	N	stuck at back
	4	Y	N	stuck at back
	6	Y	N	stuck at back
	8	Y	Y	took 3x pulses and needle rotation
8	x	Y	x	unsheathed
	2	Y	Y	took 1x pulses
9	x	Y	x	unsheathed
	2	Y	N	
	4	Y	Y	took 1x pulses
10	x	Y	x	unsheathed, peeled back
	2	Y	N	stuck at back
	4	Y	Y	took 5x pulses and needle rotation
11	x	Y	x	unsheathed
	2	Y	Y	took 1x pulses
12	x	Y	x	unsheathed, stringy
	2	N	N	heterog. piece separated and removed
	4	N	Y	took 1x pulses
13	x	Y	x	unsheathed, peeled back
	2	Y	N	stuck at back
	4	Y	N	stuck at back
	6	Y	N	stuck at back
	8	Y	Y	took 4x pulses
14	x	Y	x	unsheathed, 1/2 length
	2	Y	Y	took 3x pulses
15	x	Y	x	unsheathed, stringy
	2	Y	Y	took 4x pulses
16	x	Y	x	unsheathed, peeled back
	2	Y	Y	stuck to cartridge
	4	Y	Y	took 1x pulses
17	x	Y	x	unsheathed
	2	Y	N	stuck at back
	4	Y	Y	took 2x pulses
18	x	Y	x	unsheathed
	2	Y	Y	took 1x pulses
19	x	Y	x	unsheathed, peeled back
	2	Y	N	stuck at back
	4	Y	Y	took 2x pulses
20	x	Y	x	unsheathed
	2	Y	N	
	4	N	Y	took 1x pulses for #1, 2x pulses for #2

Run	Release Pressure (psi)
1	2
2	2
3	2
4	2
5	2
6	6
7	8
8	2
9	4
10	4
11	2
12	4
13	8
14	2
15	2
16	4
17	4
18	2
19	4
20	4

Figure AI.5 Porcine kidney CNB data

Tissue:	Pig Kidney
Fresh date:	3/31/21
Fresh time:	4:30 PM
Exp. date:	3/31/21
Exp. start time:	7:20 PM
Exp. end time:	8:25 PM
Time since fresh:	3:22
Exp. time:	1:05

Run	*P (psi)*	*Intact?*	*Removed?*	*Notes*
1	x	Y	x	unsheathed
	2	Y	N	
	4	Y	Y	took 1 pulses
2	x	Y	x	unsheathed
	2	Y	Y	took 3x pulses
3	x	Y	x	unsheathed
	2	Y	Y	took 2x pulses
4	x	Y	x	unsheathed
	2	Y	Y	took 3x pulses
5	x	Y	x	unsheathed
	2	Y	Y	took 2x pulses
6	x	Y	x	unsheathed
	2	Y	N	
	4	Y	Y	took 2x pulses
7	x	Y	x	unsheathed
	2	Y	Y	took 2x pulses
8	x	Y	x	unsheathed
	2	Y	Y	took 1x pulse
9	x	Y	x	unsheathed
	2	Y	Y	took 2x pulses
10	x	Y	x	unsheathed
	2	Y	Y	took 3x pulses
11	x	Y	x	unsheathed
	2	Y	N	off but stuck in back
	4	Y	Y	took 1x pulse
12	0	Y	x	unsheathed
	2	Y	Y	took 1x pulses
13	x	Y	x	unsheathed
	2	Y	Y	took 3x pulses
14	x	Y	x	unsheathed
	2	Y	Y	took 2x pulses
15	x	Y	x	unsheathed, 1/4 length
	2	Y	Y	took 3x pulses
16	x	Y	x	unsheathed
	2	Y	Y	took 1x pulses
17	x	Y	x	unsheathed
	2	Y	Y	took 1x pulses
18	x	Y	x	unsheathed
	2	Y	Y	took 1x pulses
19	x	Y	x	unsheathed
	2	Y	N	
	4	Y	Y	took 1x pulses
20	x	Y	x	unsheathed
	2	Y	Y	took 1x pulses

Run	Release Pressure (psi)
1	4
2	2
3	2
4	2
5	2
6	4
7	2
8	2
9	2
10	2
11	4
12	2
13	2
14	2
15	2
16	2
17	2
18	2
19	4
20	2

Figure AI.6 Porcine lung CNB data

Tissue:	Pig Lung
Fresh date:	3/31/21
Fresh time:	4:30 PM
Exp. date:	3/31/21
Exp. start time:	9:30 PM
Exp. end time:	9:55 PM
Time since fresh:	5:12
Exp. time:	0:25

Run	*P (psi)*	*Intact?*	*Removed?*	*Notes*
1	x	Y	x	unsheathed, 1/4 length
	2	Y	N	stuck at tip
	4	Y	N	stuck at tip
	6	Y	Y	took 1x pulses
2	x	Y	x	unsheathed
	2	Y	N	
	4	Y	Y	took 1x pulses
3	x	Y	x	unsheathed, came back with needle with bubbles
	2	Y	Y	took 1x pulses
4	x	Y	x	unsheathed
	2	Y	N	
	4	Y	Y	took 1x pulses
5	x	Y	x	unsheathed
	2	Y	Y	took 2x pulses
6	x	Y	x	unsheathed
	2	Y	Y	took 4x pulses
7	x	Y	x	unsheathed, 1/4 length
	2	Y	N	
	4	Y	Y	took 1x pulses
8	x	Y	x	unsheathed
	2	Y	N	
	4	Y	Y	took 1x pulses
9	x	Y	x	unsheathed, 1/4 length
	2	Y	N	
	4	Y	Y	took 2x pulses
10	x	Y	x	unsheathed
	2	Y	N	
	4	Y	N	
	6	Y	Y	took 1x pulses
11	x	Y	x	unsheathed
	2	N	Y	one half off, one half stuck at tip
	4	N	Y	both halves off
12	x	Y	x	unsheathed
	2	Y	Y	took 1x pulses
13	x	Y	x	unsheathed, many bubbles
	2	Y	Y	took 2x pulses
14	x	Y	x	unsheathed
	2	Y	Y	took 3x pulses
15	x	Y	x	unsheathed
	2	Y	Y	took 2x pulses
16	x	Y	x	unsheathed
	2	Y	Y	took 2x pulses
17	x	Y	x	unsheathed
	2	Y	N	
	4	Y	Y	took 3x pulses
18	x	Y	x	unsheathed
	2	Y	Y	took 3x pulses
19	x	Y	x	unsheathed
	2	Y	N	stuck at tip
	4	Y	Y	took 1x pulses
20	x	Y	x	unsheathed
	2	Y	Y	took 4x pulses

Run	Release Pressure (psi)
1	6
2	4
3	2
4	4
5	2
6	2
7	4
8	4
9	4
10	4
11	4
12	2
13	2
14	2
15	2
16	2
17	4
18	2
19	4
20	2

Figure AI.7 Porcine pancreas CNB data

Tissue:	Pig Pancreas
Fresh date:	3/31/21
Fresh time:	4:30 PM
Exp. date:	3/31/21
Exp. start time:	8:40 PM
Exp. end time:	9:20 PM
Time since fresh:	4:30
Exp. time:	0:40

Run	*P (psi)*	*Intact?*	*Removed?*	*Notes*
1	x	Y	x	unsheathed, 1/4 length
	2	Y	N	
	4	Y	Y	took 2x pulses
2	x	Y	x	unsheathed
	2	Y	N	
	4	Y	Y	took 2x pulses
3	x	Y	N	unsheathed, came off but stuck at back
	2	Y	N	still stuck at back
	4	Y	N	still stuck at back
	6	Y	N	still stuck at back
	8	Y	N	still stuck at back
	10	Y	Y	took 1x pulses
4	x	Y	x	unsheathed
	2	Y	Y	took 1x pulses, separated in half but connected by strand
5	x	Y	x	unsheathed
	2	Y	Y	took 1x pulses
6	x	Y	x	unsheathed
	2	Y	Y	took 1x pulses
7	x	Y	x	unsheathed
	2	Y	Y	took 1x pulses
8	x	Y	x	unsheathed
	2	Y	Y	took 1x pulses
9	x	N	x	unsheathed
	2	N	Y	took 1x pulses
10	x	Y	x	unsheathed
	2	Y	Y	took 2x pulses
11	x	Y	x	unsheathed
	2	Y	N	
	4	Y	N	
	6	Y	N	
	8	Y	Y	took 2x pulses
12	x	N	x	unsheathed, lots of bubbles
	2	N	Y	took 1x pulses
13	x	Y	x	unsheathed
	2	Y	Y	took 3x pulses
14	x	Y	x	unsheathed
	2	Y	Y	took 4x pulses
15	x	Y	x	unsheathed, 1/4 length
	2	Y	N	
	4	Y	Y	took 3x pulses
16	x	Y	x	unsheathed, 1/4 length
	2	Y	N	
	4	Y	Y	took 2x pulses
17	x	Y	x	unsheathed
	2	N	Y	clump got stuck to top of cartridge
18	x	Y	x	unsheathed, rolled back and off with needle cover
	2	Y	N	
	4	Y	N	
	6	Y	Y	took 1x pulses
19	x	Y	x	unsheathed
	2	Y	N	mostly off, stuck at end
	4	Y	N	mostly off, stuck at end
	6	Y	Y	took 1x pulses
20	x	Y	x	unsheathed
	2	Y	Y	took 1x pulses

Run	Release Pressure (psi)
1	4
2	4
3	10
4	2
5	2
6	2
7	2
8	2
9	2
10	2
11	8
12	2
13	2
14	2
15	4
16	4
17	2
18	6
19	6
20	2

Figure AI.8 Needle gauge experimental data

Experimental results of the biopsy removal module in the fully integrated cartridge (Main Chip V11). Only available gauges (14-18) were used. Need <14g and >18g in future!
All biopsies are of refrigerated (21 days) porcine kidney taken with a Bard MaxCore core needle gun (side cut).
For removal, 4 pulses of Hi Flow PBS are applied (max 3x) starting at 2.0 psi and increased in increments of 2 psi until removed.
Record all relevant observations.

Date 4/23/21
Tissue Kidney
Resection 4/2/21

Gauge	N	Released?	Intact?	Removal PSI		Notes
				1st Section	All	
14	1	Y	Y	2	2	
14	2	Y	Y	2	2	
14	3	Y	Y	6	6	NOT FULL, PEELED FROM BACK AT 4PSI,
14	4	Y	Y	8	8	VERY LITTLE TISSUE, STRINGY, PIECE IN BACK, HAD TO SPIN NEEDLE
14	5	Y	Y	4	4	
14	6	Y	Y	4	4	FULL BIOPSY
14	7	Y	Y	4	4	
14	8	Y	Y	2	2	1/2 LENGTH
14	9	Y	N	2	4	1/2 LENGTH
14	10	Y	Y	2	2	

Gauge	N	Released	Intact	Avg PSI - 1st	Med PSI - 1st	StDev - 1st	Avg PSI - all	Med PSI - all	StDev - all
14	10	10	9	3.60	3.00	2.07	3.80	4.00	1.99

Table 4. Effect of needle size on biopsy removal in the millifluidic cartridge.

Needle Gauge	N	Removed from Needle	Biopsy Stayed Intact	PSI		
				Mean	Median	St Dev
14	10	100%	100%	3.60	3.00	2.07
16	10	100%	100%	3.20	3.00	1.40
18	10	100%	80%	5.40	5.00	2.67

All CNBs, which are of refridgerated (21 days) porcine kidney were removed from their needle regardless of needle size. There is no difference in removal pressure between 14 and 16 gauge, but 18 gauge (smaller diameter) requires a larger bottle pressure to remove the CNB.

Gauge	N	Released?	Intact?	Removal PSI		Notes
				1st Section	All	
16	1	Y	N	2	2	IN HALVES AT START (NOT INTACT)
16	2	Y	Y	6	6	FULL LENGTH
16	3	Y	N	2	4	NOT INTACT AT START
16	4	Y	Y	4	4	FULL LENGTH
16	5	Y	Y	4	4	FULL LENGTH
16	6	Y	Y	2	2	2/3 LENGTH, SMALL BUBBLES
16	7	Y	N	2	8	NOT INTACT AT START - DUE TO HETEROGENEITY
16	8	Y	Y	4	4	WAS STUCK AT BACK - REQUIRED NEEDLE SPINNING
16	9	Y	Y	2	2	
16	10	Y	Y	4	4	FULL LENGTH

Gauge	N	Released	Intact	Avg PSI - 1st	Med PSI - 1st	StDev - 1st	Avg PSI - all	Med PSI - all	StDev - all
16	10	10	7	3.20	3.00	1.40	4.00	4.00	1.89

Gauge	N	Released?	Intact?	Removal PSI		Notes
				1st Section	All	
18	1	Y	Y	4	4	1/2 LENGTH, IN BACK
18	2	Y	Y	4	4	SMALL (1/6 LENGTH), "FLIMSY"
18	3	Y	Y	8	8	1/2 LENGTH, STUCK IN BACK, TOOK NEEDLE SPINNING
18	4	Y	N	8	8	STUCK AT BACK, SEPARATED IN HALF AT 8PSI PULSE 1, BACK LEFT AT PUL
18	5	Y	Y	10	10	STUCK AT BACK - REQ SPINNING
18	6	Y	Y	2	2	AT FRONT OF NEEDLE (1/2 LENGTH)
18	7	Y	Y	4	4	
18	8	Y	Y	6	6	
18	9	Y	N	2	6	BACK HALF PEELED UP AND SEPARATED AT 2PSI
18	10	Y	Y	6	6	

Gauge	N	Released	Intact	Avg PSI - 1st	Med PSI - 1st	StDev - 1st	Avg PSI - all	Med PSI - all	StDev - all
18	10	10	8	5.40	5.00	2.67	5.80	6.00	2.39

Appendix II – BT-474 Cell Culture and Staining Calculations

Figure AII.1 Cell culture subculture calculations

Container Type	Container Number	Seeding Density	Cells at Confluency	Cells during Subculture
Flask	*T-75*	2.10E+06	8.40E+06	6.30E+06
Petri-dish	*35mm*	3.00E+05	1.20E+06	9.00E+05
Well-plate	*96-well*	1.00E+04	4.00E+04	3.00E+04

CONTAIN. *IN USE*	CONTAIN. # *IN USE*	AVAILABLE CELLS
Flask	T-75	6.30E+06

SUBCULTURING QUANTITIES

# of containers	Cells per container	Total # Cells	Testing?	Cells left for passaging	% left from total	Split Ratio (1:X)
3	6.30E+06	1.89E+07	YES	6.30E+06	33.33%	3

IF TESTING (PER TEST)

Cells needed	Containers needed	Total Cells
1.00E+07	1.6	1.00E+07

Figure AII.2 Cell staining calculations

Intended Score	Trastuzumab (µg)	Theor. Her2	CPN-Ab Conj. (µg/mL)	CPN per test (µg)	% of Total CPN	Tests Possible
1+	4.592	1.00E+12	4	0.8	1.60%	62

Total Surface Cells	Total Surface Her2
4.85E+04	9.69E+10

Culture or CNB?	Total Cells	Total # Her2	Intended # Her2	# Her2 to block
Culture	1.00E+07	2.00E+13	1.00E+12	1.90E+13

Avg Cell Diameter (µm)	Avg Cell Vol (µm^3)	Total Vol Cells (mm^3)	Total Radius (mm)	Tot. SA (mm^2)	Tot. Surf. Cells	Tot. Surf. Her2
15	235.619449	2.3562	0.8255	8.562979058	4.85E+04	9.69E+10

Mass Trast. (g/mol)	# Trast per gram	Needed Trast. (g)
145531.86	4.13802E+18	4.59E-06

Mass CPN (g/mol)	# CPN per gram	Diameter CPN (nm)	SA CPN (nm^2)	Size CPN (nm)
6.0221E+10	1.00E+13	80	20106.19298	70-80

Mass CB11 Ab (g/mol)	Width CB11 Ab (nm)	Max CB11 per CPN
150000	14.5	346

Mass CPN-Ab (g/mol)	CPN-Ab per gram	Needed CPN-Ab (µg)	Needed # CPN-Ab	Mass CPN-Ab (kDa)
6.0273E+10	9.9914E+12	5,004.31	5.00E+10	6.0273E+07

Conc CPN-Ab (mg/mL)	Purchase Vol (mL)	Purchase Mass (µg)
0.1	0.5	50

1. # of cells in surface layer of CNB:

CNB diameter (mm)	CNB length (mm)	CNB Surface Area (mm^2) [1]
1.628	10	51.14362

Cell Diameter (mm)	Area of Hexagon w/ 7 cells (mm^2) [2]			Hexagons per CNB		# of surface cells per CNB
0.02	0.00233826859	/ CNB SA	=	21872.43168	x7cells/hex =	153107.0218

Appendix III – Miscellaneous Figures

Figure AIII.1 Quartz is better than sapphire in MUSE imaging

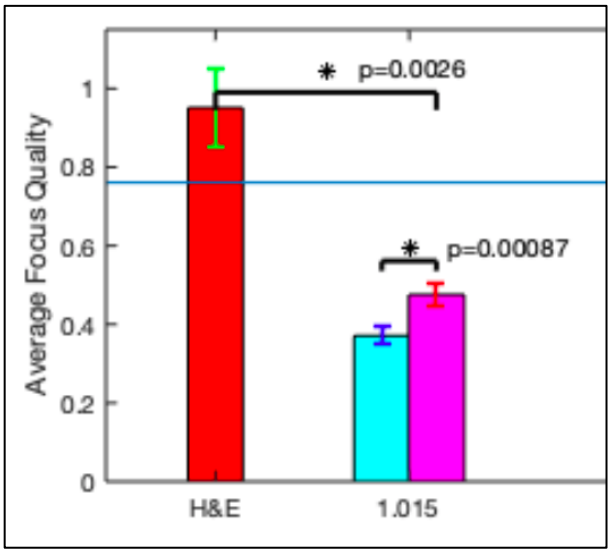

Figure AIII.2 MUSE image of a blank coverslip

Appendix IV – NW Biospecimen Documents

Document IV.1 Exempt Determinations Worksheet

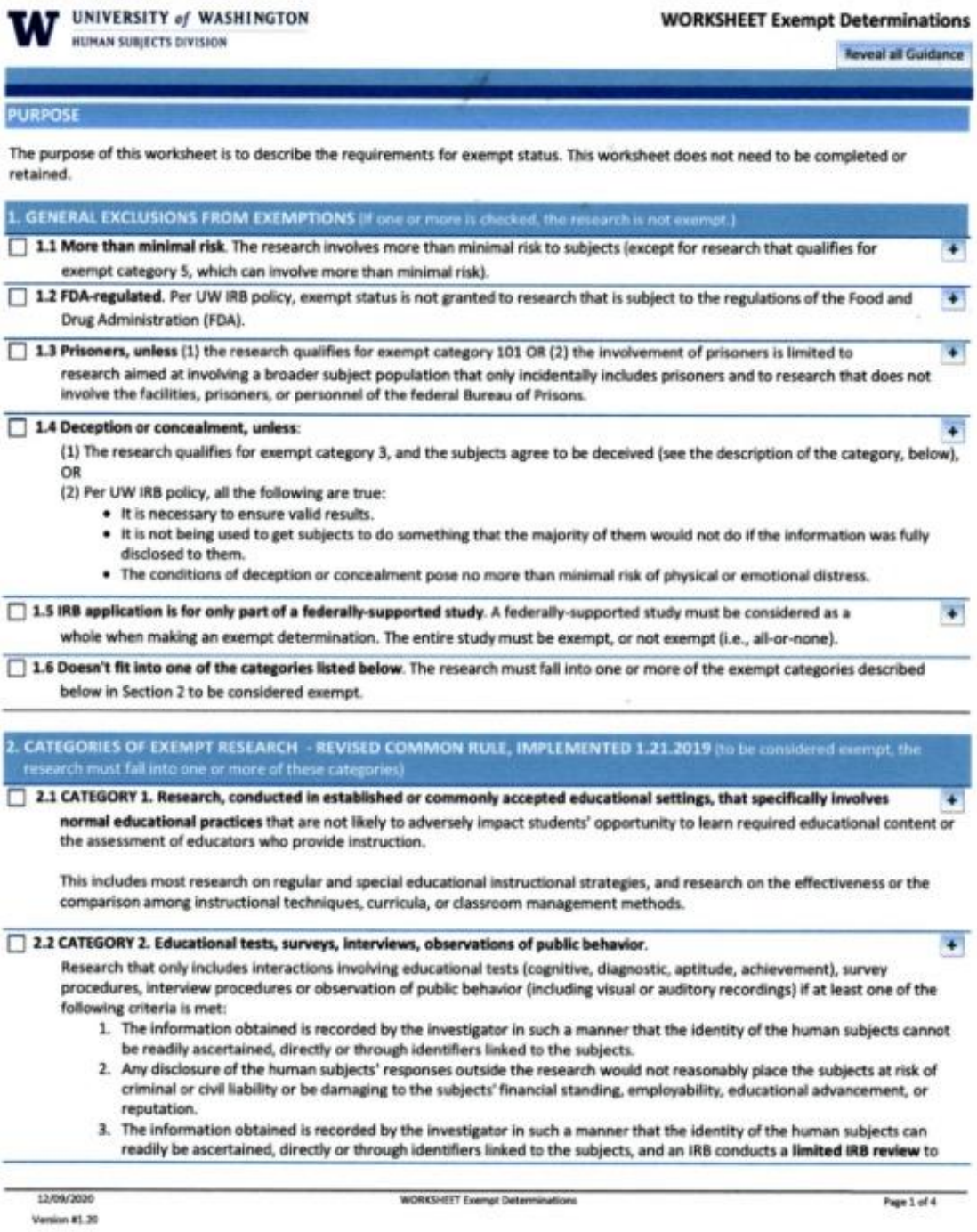

UNIVERSITY of WASHINGTON
HUMAN SUBJECTS DIVISION

WORKSHEET Exempt Determinations

Reveal all Guidance

PURPOSE

The purpose of this worksheet is to describe the requirements for exempt status. This worksheet does not need to be completed or retained.

1. GENERAL EXCLUSIONS FROM EXEMPTIONS (If one or more is checked, the research is not exempt.)

☐ **1.1 More than minimal risk.** The research involves more than minimal risk to subjects (except for research that qualifies for exempt category 5, which can involve more than minimal risk).

☐ **1.2 FDA-regulated.** Per UW IRB policy, exempt status is not granted to research that is subject to the regulations of the Food and Drug Administration (FDA).

☐ **1.3 Prisoners, unless** (1) the research qualifies for exempt category 101 OR (2) the involvement of prisoners is limited to research aimed at involving a broader subject population that only incidentally includes prisoners and to research that does not involve the facilities, prisoners, or personnel of the federal Bureau of Prisons.

☐ **1.4 Deception or concealment, unless**:
(1) The research qualifies for exempt category 3, and the subjects agree to be deceived (see the description of the category, below), OR
(2) Per UW IRB policy, all the following are true:
- It is necessary to ensure valid results.
- It is not being used to get subjects to do something that the majority of them would not do if the information was fully disclosed to them.
- The conditions of deception or concealment pose no more than minimal risk of physical or emotional distress.

☐ **1.5 IRB application is for only part of a federally-supported study.** A federally-supported study must be considered as a whole when making an exempt determination. The entire study must be exempt, or not exempt (i.e., all-or-none).

☐ **1.6 Doesn't fit into one of the categories listed below.** The research must fall into one or more of the exempt categories described below in Section 2 to be considered exempt.

2. CATEGORIES OF EXEMPT RESEARCH - REVISED COMMON RULE, IMPLEMENTED 1.21.2019 (to be considered exempt, the research must fall into one or more of these categories)

☐ **2.1 CATEGORY 1. Research, conducted in established or commonly accepted educational settings, that specifically involves normal educational practices** that are not likely to adversely impact students' opportunity to learn required educational content or the assessment of educators who provide instruction.

This includes most research on regular and special educational instructional strategies, and research on the effectiveness or the comparison among instructional techniques, curricula, or classroom management methods.

☐ **2.2 CATEGORY 2. Educational tests, surveys, interviews, observations of public behavior.**
Research that only includes interactions involving educational tests (cognitive, diagnostic, aptitude, achievement), survey procedures, interview procedures or observation of public behavior (including visual or auditory recordings) if at least one of the following criteria is met:
1. The information obtained is recorded by the investigator in such a manner that the identity of the human subjects cannot be readily ascertained, directly or through identifiers linked to the subjects.
2. Any disclosure of the human subjects' responses outside the research would not reasonably place the subjects at risk of criminal or civil liability or be damaging to the subjects' financial standing, employability, educational advancement, or reputation.
3. The information obtained is recorded by the investigator in such a manner that the identity of the human subjects can readily be ascertained, directly or through identifiers linked to the subjects, and an IRB conducts a **limited IRB review** to

12/09/2020 WORKSHEET Exempt Determinations Page 1 of 4
Version #1.20

make the determination that, when appropriate, there are adequate provisions to protect the privacy of subjects and to maintain the confidentiality of data.

Research involving children does not qualify for this exempt category if: (1) the research involves surveys, interviews, and/or observations of public behavior when the research team participates in the activities being observed, or (2) if Limited IRB Review is required.

☐ **2.3 CATEGORY 3. Benign behavioral interventions.** Research involving benign behavioral interventions in conjunction with the collection of information from an adult subject through verbal or written responses (including data entry) or audiovisual recording if the subject prospectively agrees to the intervention and information collection and at least one of the following criteria is met:

A. The information obtained is recorded by the investigator in such a manner that the identity of the human subjects cannot readily be ascertained, directly or through identifiers linked to the subjects;
B. Any disclosure of the human subjects' responses outside the research would not reasonably place the subjects at risk of criminal or civil liability or be damaging to the subjects' financial standing, employability, educational advancement, or reputation; or
C. The information obtained is recorded by the investigator in such a manner that the identity of the human subjects can readily be ascertained, directly or through identifiers linked to the subjects, and an IRB conducts a **limited IRB review** to determine that the research (when appropriate) has adequate provisions to protect the privacy of subjects and to maintain the confidentiality of data.

Research involving children does not qualify for this exempt category.

☒ **2.4 CATEGORY 4. Secondary research uses of identifiable private information or identifiable biospecimens** for which consent is not required, if at least one of the following criteria is met:

1. **Publicly available**. The identifiable private information or identifiable biospecimens are publicly available.
2. **Not identifiable as recorded**. Information, which may include information about biospecimens, is recorded by the investigator in such a manner that the identity of the human subjects cannot readily be ascertained directly or through identifiers linked to the subjects, the investigator does not contact the subjects, and the investigator will not re-identify subjects.
3. **Use of PHI**. The research involves only information collection and analysis involving the investigator's use of identifiable health information when that use is regulated under HIPAA regulations, for the purposes of health care operations, research, or public health activities and purposes (as those purposes are described in the HIPAA regulations).
4. **Use of federally generated or collected information or biospecimens**. The research is conducted by, or on behalf of, a federal department or agency using government-generated or government-collected information originally obtained for non-research activities, if the original collection and the secondary use of the information or biospecimens occurs in compliance with three specific federal statues meant to safeguard privacy.

☐ **2.5 CATEGORY 5. Research and demonstration projects that are conducted or supported by a federal department or agency, or otherwise subject to the approval of department or agency heads** (or the approval of the heads of bureaus or other subordinate agencies that have been delegated authority to conduct the research and demonstration projects), and that are designed to study, evaluate, improve, or otherwise examine public benefit or service programs, including procedures for obtaining benefits or services under those programs, possible changes in or alternatives to those programs or procedures, or possible changes in methods or levels of payment for benefits or services under those programs.

As described in federal guidance, all of the following criteria must be satisfied.

1. The program under study delivers a public benefit or service.
2. The project must be conducted pursuant to specific federal statutory authority.
3. There must be no statutory requirement that the project be reviewed by an IRB.
4. The project does not involve significant physical invasions or intrusions upon the privacy of participants.
5. The funding agency concurs with the exemption.

NOTE: The revised Common Rule explicitly states that minimal risk is not a requirement for this exempt category.

☐ **2.6 CATEGORY 6. Taste and food quality evaluation and consumer acceptance studies**: (i) if wholesome foods without

additives are consumed, or (ii) if a food is consumed that contains a food ingredient at or below the level and for a use found to be safe, or agricultural chemical or environmental contaminant at or below the level found to be safe, by the Food and Drug Administration or approved by the Environmental Protection Agency or the Food Safety and Inspection Service of the Department of Agriculture.

The UW does not currently grant exempt status in the following category but the description is provided here for informational purposes.

☐ **2.7 CATEGORY 7. Storage or maintenance for secondary research for which broad consent is required**. Storage or maintenance of identifiable private information or identifiable biospecimens for potential secondary research use if an IRB conducts a limited IRB review and makes all of the following determinations.

1. Broad consent for storage, maintenance, and secondary research use of identifiable private information or identifiable biospecimens is obtained in accordance with the following requirements:
    a. Broad consent is obtained from the subject or the subject's legally authorized representative.
    b. Circumstances provide the prospective subject or the legally authorized representative sufficient opportunity to discuss and consider whether or not to participate and that minimize the possibility of coercion or undue influence.
    c. The information given to the subject or legally authorized representative is in language understandable to the subject or legally authorized representative.
    d. The prospective subject or legally authorized representative are provided with the information that a reasonable person would want to have in order to make an informed decision about whether to participate, and an opportunity to discuss that information.
    e. The consent does not include any exculpatory language through which the subject or legally authorized representative is made to waive or appear to waive any of the subject's legal rights, or releases or appears to release the investigator, the sponsor, the institution or its agents from liability for negligence.
    f. The following information will be provided to the subject or legally authorized representative:
        i. A description of any reasonably foreseeable risks or discomforts to the subject.
        ii. A description of any benefits to the subject or to others that may reasonably be expected from the research.
        iii. A statement describing the extent, if any, to which confidentiality of records identifying the subject will be maintained.
        iv. A statement that participation is voluntary, refusal to participate will involve no penalty or loss of benefits to which the subject is otherwise entitled, and the subject may discontinue participation at any time without penalty or loss of benefits to which the subject is otherwise entitled.
        v. (If appropriate) A statement that the subject's biospecimens (even if identifiers are removed) may be used for commercial profit and whether the subject will or will not share in this commercial profit.
        vi. (If appropriate) For research involving biospecimens, whether the research will (if known) or might include whole genome sequencing (i.e., sequencing of a human germline or somatic specimen with the intent to generate the genome or exome sequence of that specimen).
        vii. A general description of the types of research that may be conducted with the identifiable private information or biospecimens. This must include sufficient information such that a reasonable person would expect that the broad consent would permit the types of research conducted.
        viii. A description of the identifiable private information or biospecimens that might be used in research, whether sharing of identifiable private information or biospecimens might occur, and the types of institutions or researchers that might conduct research with the identifiable private information or biospecimens.
        ix. A description of the period of time that the identifiable private information or biospecimens may be stored and maintained (which period of time could be indefinite), and a description of the period of time that the identifiable private information or biospecimens may be used for research purposes (which period of time could be indefinite).
        x. Unless the subject or legally authorized representative will be provided details about specific research studies, a statement that they will not be informed of the details of any specific research studies that might be conducted using the subject's identifiable private information or biospecimens, including the purposes of the research, and that they might have chosen not to consent to some of those specific research studies.
        xi. Unless it is known that clinically relevant research results, including individual research results will be disclosed to the subject in all circumstances, a statement that such results may not be disclosed to the subject.

xii. An explanation of whom to contact for answers to questions about the subject's rights and about storage and use of the subject's identifiable private information or identifiable biospecimens, and whom to contact in the event of a research-related harm.

2. Broad consent is appropriately documented or waiver of documentation is appropriate.
3. If there is a change made for research purposes in the way the identifiable private information or identifiable biospecimens are stored or maintained, there are adequate provisions to protect the privacy of subjects and to maintain the confidentiality of data.

NOTE: This requires:

- Recording and tracking of who has agreed to or refused the broad consent.
- Tracking the terms of the broad consent to determine whether proposed future secondary research use falls within the scope of the identified types of research and circumstance of the use.

The UW does not currently grant exempt status in the following category but the description is provided here for informational purposes.

☐ **2.8 CATEGORY 8. Secondary research for which broad consent is required**. Research involving the use of identifiable private information or identifiable biospecimens for secondary research use, if all of the following criteria are met.

1. Broad consent for the storage, maintenance, and secondary research use of the identifiable private information or biospecimens was obtained in accordance with all of the requirements described for exempt category 7.
2. Documentation of informed consent or waiver of documentation of consent was obtained.
3. An IRB conducts a limited IRB review and makes the following determinations:
   a. When appropriate, there are adequate provisions to protect the privacy of subjects and to maintain the confidentiality of the data.
   b. The research to be conducted is within the scope of the broad consent provided by the subjects.
4. The investigator does not include returning individual research results to subjects as part of the study plan. (Note: this provision does not prevent an investigator from abiding by any legal requirements to return individual research results.)

☐ **2.101 CATEGORY 101. Non-federally-supported research** in which:

- Subjects are cognitively-competent **adults**, AND
- Research procedures consist solely of benign interventions, interactions, or observations of behavior, AND
- No biological specimens are being collected, AND
- The physical assessment of subject's physical characteristics is limited to standard anthropometrics and vital signs, AND
- The information obtained is recorded in such a manner that the human subjects cannot be identified, directly or through identifiers linked to the subjects; OR, if subjects can be identified, any disclosure of the human subjects' responses outside the research could not reasonably place the subjects at risk of criminal or civil liability or be damaging to the subjects' financial standing, employability, educational advancement, or reputation.

Research involving children does not qualify for this exempt category.

Document AIV.2 Research Proposal

A novel biomarker and imaging system for the fresh analysis of HER2 in breast cancer core needle biopsies

David Cooper

April 14, 2020 | Human Photonics Laboratory | Master's Thesis Proposal

Background & Significance

HER2 Breast Cancer Classification

Each year, around 230,000 people in the United States are diagnosed with invasive breast cancer[1]. Of these, approximately 15-20% of these cancers are found to be HER2 positive (HER2+). HER2+ breast cancer, also known as IHC 3+, is defined, by the ASCO/CAP 2013 recommendations, as having uniform intense (HER2) membrane staining in more than 10% of invasive tumor cells in a sample. This classification is the highest of the three HER2 statuses and is the only one that receives HER2-specific treatment. The status below HER2+ is HER2 equivocal, also known as IHC 2+, which is defined as having incomplete or weak membrane staining in >10% of cells or intense membrane staining in ≤10% of cells. The lowest HER2 classification is HER2 negative (HER2-), which contains IHC 1+ and IHC 0 scores. IHC 1+ is defined as having faint incomplete membrane staining in >10% of cells and IHC 0 is defined as having no staining or faint staining in ≤10% of cells.

Current Problems with HER2 IHC

HER2 status in breast cancer tumors can be diagnosed using many methods, but immunohistochemistry (IHC) assays are the most common. HER2 IHC is a technique that tags the HER2 protein receptor with a fluorescent probe for optical imaging and is easy to perform. Unfortunately, due to the inability to amplify proteins, IHC is subjective because it is limited by what is present in the sample and/or what the imaging marker can detect. Patients diagnosed with HER2+ breast cancer undergo specialized HER2-targeting treatments that greatly improve their outcome but have a detrimental effect or no effect on HER2- cancers. Therefore, only IHC 3+ breast cancer patients are given the beneficial HER2-targeted treatment even though HER2+ cancer may have been misdiagnosed as IHC 1+ or 2+. Furthermore, traditional HER2 markers used in IHC, which are typically anti-HER2 monoclonal antibodies conjugated to conventional organic dyes, make the detection and diagnosis of early stage HER2+ breast cancer very difficult[2] due to their lower specificity and sensitivity. Although solutions to replace IHC with more sensitive methods have been proposed, there is much opposition from pathologists and pathology labs. Additionally, many methods to increase the sensitivity of IHC, such as using quantum dots instead of conventional fluorophores, have been proposed and studied. Unfortunately, none of these studies have researched their solution in fresh tissue samples using deep-UV light to excite the staining molecules. These specifications are necessary for the inclusion of HER2 IHC in CoreView, a novel automated histopathology device, being developed in my lab, that uses microscopy with ultraviolet surface excitation (MUSE) to stain and image the surface of fresh core needle biopsies (CNBs) to aid in a quicker and more accurate diagnosis of cancers[3-4].

Hypothesis

CB11-CPN680, a custom primary anti-HER2 antibody conjugated polymer nanoparticle, can be used to improve the sensitivity of HER2 IHC in fresh breast cancer CNBs.

Rationale

CPN680 [Stream Bio] is a conjugated polymer nanoparticle (CPN) that is UV-excitable and emits a red color (680 nm). CPN680 was chosen over other CPNs because it is the closest color to the reddish-brown emission of traditional HER2 IHC stains. CPNs will increase IHC sensitivity because they are 100-1000x brighter than Quantum dots and Qbeads, which are already significantly brighter than traditional IHC stains[5]. These CPNs are conjugated to CB11 [Abcam], a primary anti-HER2 antibody commonly used in HER2 IHC. This novel CB11-CPN680 marker cannot be used in all applications because it is too large (~80 nm) to diffuse through the plasma membrane of live cells and will be somewhat resistant to intercellular diffusion. CB11-CPN680 will, however, work in CoreView because MUSE is restricted to imaging only the first few layers of cells and HER2 is an extracellular receptor.

Specific Aims & General Approach

Specific Aim 1: Confirm the improved sensitivity and specificity of the CB11-CPN680 marker in CoreView/MUSE-based HER2 IHC using BT-474 human breast cancer cell line culture.
General Approach 1: BT-474 human breast cancer cells (HER2+, PR+, ER-, CK5/6-, EGFR+) will be indefinitely cultured using standard mammalian cell culture techniques to provide HER2+ cell pellets for imaging. HER2 classification will be effectively controlled using Trastuzumab, an anti-HER2 antibody to block a specified number of HER2 receptors. Trastuzumab-bound HER2 receptors will not be available for CB11-CPN680 binding and will therefore be undetected by the CoreView/MUSE-based HER2 IHC. All cell pellets will be imaged using a MUSE imaging platform, and HER2 classification will be determined by a collaborating pathologist. HER2 classification will be confirmed using traditional IHC in a collaborating pathology lab.

Specific Aim 2: Confirm the improved sensitivity and specificity of the CB11-CPN680 marker in CoreView/MUSE-based HER2 IHC using fresh human breast cancer samples.
General Approach 2: All methods from ***General Approach 1*** will be repeated using fresh human breast cancer samples with known HER2 classifications provided by NW BioTrust. All samples will have no identifying information, with the exception of HER2 classification. The goal is to have 15 samples of each HER2 classification (IHC 3+, 2+, 1+, and 0), but Trastuzumab can be used if HER2 equivocal or HER2- samples are unavailable. As HER2 IHC staining has been shown to be reduced by cold ischemic time, all samples must be analyzed and fixed in formalin within 4 hours (if cold) or 2 hours (if warm) of biopsy acquisition[1].

Citations

1. Nitta H., Kelly D., Allred C., Jewell S. Peter B., Dennis E., & Grogan T.M. "The assessment of HER2 status in breast cancer: the past, the present, and the future." *Path. Int.* 2016; 66: 313-324. doi:10.1111/pin.12407
2. Rakovich T.Y., et al. "Highly sensitive single domain antibody-quantum dot conjugates for detection of HER2 biomarker in lung and breast cancer cells." *ACS Nano.* 2014; 8(6): 5682-95. doi:10.1021/nn500212h
3. Xie W., et al. "Microscopy with ultraviolet surface excitation for wide-area pathology of breast surgical margins." *J. Biomed. Opt.* 2019; 24(2). doi:10.1117/1.JBO.24.2.026501
4. Cooper D.J., Fauver M.E., Dintzis S.M., & Seibel E.J. "Rapid needle biopsy assessment at point of care to advance personalized cancer therapy [abstract]." In: Proceedings of the Annual Meeting of the American Association for Cancer Research 2020; 2020 Apr 27-28 and Jun 22-24. Philadelphia (PA): *AACR; Cancer Res* 2020; 80(16 Suppl):Abstract nr LB-285
5. "CPN – Conjugated Polymer Nanoparticles" Stream Bio 2020. Accessed Apr 4, 2021 from: https://www.streambio.co.uk/our-technology/

Document AIV.3 Study Registration

nwbiospecimen
annotated research biospecimens

UW Medicine
UNIVERSITY OF WASHINGTON MEDICAL CENTER

UW Medicine
HARBORVIEW MEDICAL CENTER

1959 NE Pacific St., Box 356100
Seattle, WA 98195
Contact: Research Program Coordinator
Ph: 206-598-7929; Fax: 206-598-5068
nwbios@uw.edu

Research Registration Form

Please Note: There will be a registration fee, billed yearly

Principal Investigator Name: Eric Seibel	Principal Investigator Email & Phone: eseibel@uw.edu	206-616-1486
Institution, Address & Box / Room #: University of Washington, 204 Fluke Hall, Dept Mechanical Engineering, Box 352600		
City, State & Zip: Seattle, WA 98195		
Study Coordinator / Contact Name: David Cooper	Study Coordinator Email & Phone: cooper24@uw.edu	425-772-1717
Institution, Address & Box / Room #: University of Washington, 232 Fluke Hall, 4000 Mason Road		
City, State & Zip: Seattle, WA 98195		

Billing / Study Information

Billing Coordinator/ Contact: Nancy Moses	Billing Coordinator Email & Phone: 206-685-2575	☐Clinical Trial (Attach CRBB pricing page)
Institution, Address & Box / Room #: UW Dept. Mechanical Engineering, Box 352600,		
City, State & Zip: Seattle, WA 98195		
UWMC / HMC Budget Number & Name: 62-0754 ☒ Federal Funds ☐Not Federal Funds	Budget Expiration Date: 3/31/2022	☐ Check here if you do not have a budget # & need to be billed by invoice (Invoice will be sent to budget coordinator unless otherwise noted)
Study Title: A novel biomarker and imaging system for the fresh analysis of Her2 in breast cancer core needle biopsies		
Number of Expected Subjects: 60	Pathology Research Service Request Start Date: April 26, 2021	Pathology Research Service Request End Date: July 2, 2021
IRB Status: ☐Approved ☐Pending ☐Qualifies for "Non-human subject" review		IRB File Number: See letter from NW Bio Trust Determined IRB exempt (see documents)
IRB Institution: ☒UW ☐FHCRC ☐Other:		IRB Expiration Date:
☐Attach a copy of IRB application and IRB approval. *This is required to complete registration.*		
Does IRB allow receipt of identifiers, ☐No ☐yes IF yes , list study team members ok to receive: ☐Patient consent signature pages must be submitted per request OR ☐HIPPA and Consent waiver (IRB approved)		
*The CLIA holder or designee must review and approve all requests involving the use of existing patient materials before processing begins. If there is a collaborating pathologist on the study, please list the pathologist and attach a letter of support from the Collaborating Pathologist. Collaborating Pathologist: Dr. Suzanne Dintzis		
Completed by: Eric Seibel, David Cooper		Date: 4/9/2021

nwbiospecimen
annotated research biospecimens

UW Medicine
UNIVERSITY OF WASHINGTON MEDICAL CENTER

UW Medicine
HARBORVIEW MEDICAL CENTER

Detailed Study information

Request Information:

What kinds of samples are needed for your study?

- [x] Fresh tissues (surgery or biopsies) collected according to your protocol
- [ ] Blood drawn in conjunction with clinical or surgery appointments
- [ ] Materials from the CLIA archive (cores, unstained slides, stained slides, curls, etc - please reference Service Request Form)
- [ ] Stained slides
- [ ] Other:

General Population Requirements ☐ NA (study or trial identifies patient)

Patient Gender: any
Age at time of collection: any
Race/Ethnicity: any
Primary Histological Diagnosis: Her2 diagnosis (3+, 2+, 1+, 0)
BioMarker: Her2
Other:

Are there any other exclusion criteria (e.g. pregnancy, diseased states) NO

Is cancer treatment and previous treatment relevant to your study? ☐ YES ☒ NO

Are patients with prior cancer history OK?
☒ YES ☐ NO ☐ OK if _____years post therapy or _____
Are samples collected after neoadjuvant therapy OK?
☒ YES ☐ NO
Are patients with BCC or SCC OK?
☒ YES ☐ NO

Tissue Samples

Tissue Type:	**MAMMARY**	I need enough sample to take a 10 mm 14-16 gauge (~2 mm) core needle biopsy. I need all samples within 4 hours if they are placed on ice and within 2 hours if not. I am available to pick up samples almost any time/day. I would like to acquire 15 samples of each type of IHC Her2 classification (3+/positive, 2+/equivocal, 1+,0/negative) of human breast cancer samples. I heard 2+/1+ will likely be unavailable, so 3+/positive would be needed in their place (for Trastuzumab blocking – see proposal).
Anatomical site:	**BREAST**	
Minimum size:	**2 X 2 X 12 MM**	
Preferred size:	**4 X 4 X 20 MM**	

Appendix V – Predictive HER2 IHC Single Frame Results

Table AV – Predictive HER2 IHC Statistics and Results

Image Frame	CPN Cells	Nuclei	% Cells w/ CPN	Average Uniformity	HER2 Score/Status		
					Prediction	Diagnosis	Known
1.2.1	22	1858	1.18%	8%	0	U	
1.2.4	68	1282	5.30%	29%	0	U	
2.1.2	6	3390	0.18%	13%	0	0	NEG
2.1.4	5	4161	0.12%	41%	0	0	NEG
2.1.6	4	4398	0.09%	27%	0	0	NEG
2.2.2	5	4009	0.12%	6%	0	0	NEG
2.2.4	5	3997	0.13%	5%	0	0	NEG
2.2.6	5	2195	0.23%	19%	0	0	NEG
3.1.5	45	2033	2.21%	15%	0	0	NEG
3.1.13	22	2505	0.88%	11%	0	0	NEG
3.1.19	4	2180	0.18%	2%	0	0	NEG
3.2.4	7	2079	0.34%	5%	0	0	NEG
3.2.12	5	2549	0.20%	2%	0	0	NEG
3.2.14	13	1687	0.77%	31%	0	0	NEG
4.1.8	37	636	5.82%	20%	0	0	NEG
4.1.28	40	1528	2.62%	24%	0	0	NEG
4.1.34	32	1865	1.72%	13%	0	0	NEG
4.2.30	104	1101	9.45%	17%	1+	U	NEG
4.2.32	113	1739	6.50%	26%	0	U	NEG
4.2.44	66	526	12.55%	24%	2+	U	NEG
5.1.23*	114	912	12.50%	14%	1+	0	NEG
5.1.64*	142	986	14.40%	11%	1+	0	NEG
5.1.98*	51	926	5.51%	15%	0	NEG	NEG
6.1.16	8	2211	0.36%	23%	0	0	NEG
6.1.18	7	1976	0.35%	5%	0	0	NEG
6.1.22	7	2421	0.29%	10%	0	0	NEG
6.2.13	9	924	0.97%	15%	0	0	NEG
6.2.15	12	1117	1.07%	16%	0	0	NEG
6.2.20	9	986	0.91%	11%	0	0	NEG
6.3.14	10	1296	0.77%	12%	0	0	NEG
6.3.22	29	712	4.07%	20%	0	0	NEG
6.3.25	11	1451	0.76%	7%	0	0	NEG

Figure AV.1

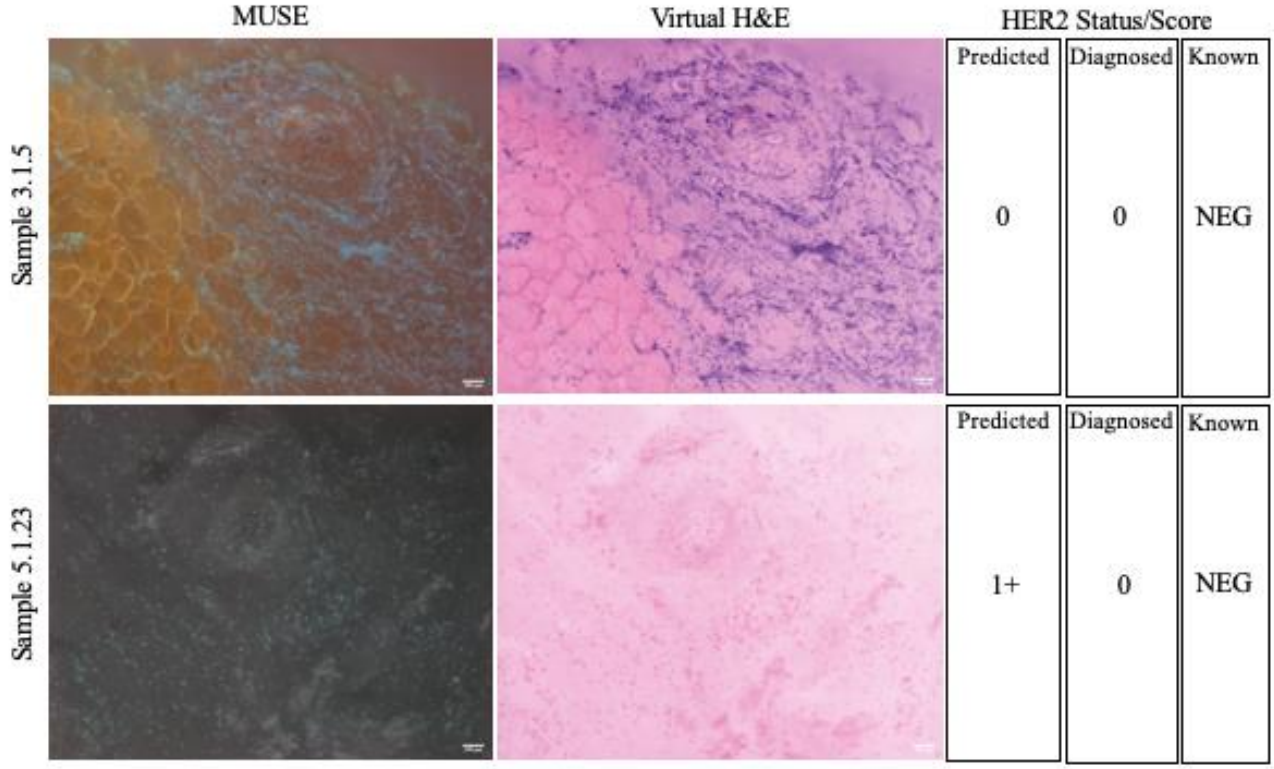

A visual comparison of Sample 3.1 and 5.1, showing the need for cytoplasmic staining with Rhodamine B. Sample 5.1 cannot reliably be interpreted by my prediction plugin nor Dr. Dintzis, but it showed that Rhodamine B was not impacting CPN680 detection with the plugin.

Appendix VI – Dr. Dintzis' Evaluations and Diagnoses (Full Results)

Figure AVI.1 – Dr. Dintzis' MUSE/Virtual H&E Evaluations

Triage Rank	Sample	Frame	Interpretable? (Y/N)	Cancer? (Y/N)	Breast Cells? (Y/N)	HER2 Status (P/N)	HER2 Score (0-3+)	Notes
11	1.1	2						weak membranous staining
12	1.2	1						weak membranous staining
		4						foci of moderate membranous staining, high background, not circumferential
9	2.1	2			n		0	increased cellularity but insufficient detail for histologic dx
		4			n		0	increased cellularity but insufficient detail for histologic dx
		6			n		0	increased cellularity but insufficient detail for histologic dx
10	2.2	2			n		0	increased cellularity but insufficient detail for histologic dx
		4			n		0	increased cellularity but insufficient detail for histologic dx
		6			n		0	increased cellularity but insufficient detail for histologic dx
7	3.1	5			n		0	circular artefact not entirely in plane of focus; ? adipose tissue with high background?
		13			n		0	circular artefact not entirely in plane of focus; ? adipose tissue with high background?
		19			n		0	circular artefact not entirely in plane of focus; ? adipose tissue with high background?
		PANO						
8	3.2	4			n		0	increased cellularity but insufficient detail for histologic dx
		12			n		0	increased cellularity but insufficient detail for histologic dx
		14			n		0	circular artefact not entirely in plane of focus; ? adipose tissue with high background?
		PANO						
5	4.1	8			n		0	increased cellularity but insufficient detail for histologic dx
		28			n		0	"
		34			n		0	"
		PANO						
6	4.2	30						weak membranous staining
		32						weak membranous staining
		44						circular artefact not entirely in plane of focus; ? adipose tissue with high background?
		PANO						
16	5.1	23			n		0	
		64			n		0	
		98			n			
		PANO						
13	6.1	16			n		0	increased cellularity but insufficient detail for dx
		18			n		0	increased cellularity but insufficient detail for dx
		22			n		0	increased cellularity but insufficient detail for dx
		PANO						
14	6.2	13			n		0	increased cellularity
		15			n		0	high cytoplasmic background
		20			n		0	increased cellularity
		PANO						
15	6.3	14			n		0	high cytoplasmic background and ? fat
		22			n		0	high cytoplasmic background
		25			n		0	
		PANO						
3	FFPE HER2+ Slide 1	3						
		31						
		39						
2	FFPE HER2+ Slide 2	9						
		23						
		44						
		PANO						
4	FFPE HER2- Slide 1	10						
		14						
		39						
		PANO						
1	FFPE HER2- Slide 2	PANO						

Figure AVI.2 – Dr. Dintzis' Standard Histopathology Evaluations

Sample	Type	Location in NDP.serve	Interpretable? (Y/N)	Cancer? (Y/N)	Breast Cells? (Y/N)	HER2 Status (P/N)	HER2 Score (0-3+)	Notes
1	H&E	ESeibel > 21-H357 > H&E	y	y	y	x	x	
	IHC	ESeibel > 21-H357 > CB11 HER2	y	y	y	n	1+	
2.1	H&E	ESeibel > 21-H357	y (see comment)	?	y	x	x	fibroinflammatory vs spindle cell carcinoma, would need to do stains to determine nature of lesion
	IHC	ESeibel > 21-H357 > CB11 HER2	y (see comment)	?	y	n	0	
2.2	H&E	ESeibel > 21-H357 > H&E	y (see comment)	?	y	x	x	fibroinflammatory vs spindle cell carcinoma, would need to do stains to determine nature of lesion
	IHC	ESeibel > 21-H357 > CB11 HER2	y (see comment)	?	y	n	0	
2.3	H&E	ESeibel > 21-H357 > H&E	Y (see comment)	?	y	x	x	fibroinflammatory vs spindle cell carcinoma, would need to do stains to determine nature of lesion
	IHC	ESeibel > 21-H357 > CB11 HER2	y	?	y	n	0	
3.1	H&E	ESeibel > 21-H424	y	y	y	x	x	
	IHC	ESeibel > 21-H357 > CB11 HER2	y	y	y	n	0	
3.2	H&E	ESeibel > 21-H424	y	y	n	x	x	
	IHC	ESeibel > 21-H357 > CB11 HER2	y	y	n	n	0	
3.3	H&E	ESeibel > 21-H424	y	y	n	x	x	
	IHC	ESeibel	y	y	n	n	0	
4.1	H&E	ESeibel > 21-H424	y	y	y	x	x	
	IHC	ESeibel	y	y	y	n	0	
4.2	H&E	ESeibel > 21-H424	y	y	n	x	x	
	IHC	ESeibel	y	y	n	n	0	
115241#5	IHC	ESeibel > 21-H489	y	y	n	n	0	nuclear staining present. No membranous staining identified
115242#5	IHC	ESeibel > 21-H489	y	y	n	n	0	nuclear staining present. No membranous staining identified
115241#2	IHC	ESeibel > 21-H489	y	y	n	n	0	background stromal staining, cancer cells are negative
115242#2	IHC	ESeibel > 21-H489	y	y	n	n	0	background stromal staining, cancer cells are negative
115241#1	IHC	ESeibel > 21-H489	y	y	y	n	0	
115242#2	IHC	ESeibel > 21-H489	y	y	n	n	0	background stromal staining, cancer cells are negative

Appendix VII – Antigen Retrieval Full Methods

Figure AVII.1 – Antigen Retrieval Google Sheet

Steps

1	**Deparaffination**
1.1	Heat the slide at 55ºC for 10 min to melt wax
1.2	Xylene for 5 min x 2
1.3	1:1 Xylene:100% EtOH for 5 min
1.4	100% EtOH for 5 min x 2
1.5	95% EtOH for 5 min
1.6	70% EtOH for 5 min
1.7	50% EtOH for 5 min
1.8	DI Water for 5 min x 2
2	**Antigen Retrieval**
2.1	Overlap slide with another (image)
2.2	Immerse in 95ºC Citrate Buffer for 15 min
2.3	Cool in water for 10 min
2.4	Remove paper clip and slide
3	**Staining**
3.1	Pipette 50mL of CPN solution onto slide, stain 30 min
3.2	Immerse in PBS to rinse for 10 s
3.3	Pipette 50mL of H&RB solution onto slide, stain 10 min
3.4	Immerse in PBS to rinse for 30 s
3.5	Place quartz coverslip on top for imaging

from https://www.ncbi.nlm.nih.gov/pmc/articles/PMC4845152/

https://www.abcam.com/protocols/ihc-deparaffinization-protocol

https://www.thermofisher.com/us/en/home/life-science/protein-biology/protein-biology-learning-center/protein-biology-resource-library/pierce-protein-methods/paraffin-removal-antigen-retrieval.html